Structure of β-decay strength functions

Yu. V. Naumov, A. A. Bykov, and I. N. Izosimov

Scientific-Research Institute of Physics, Leningrad State University
Fiz. Elem. Chastits At. Yadra **14**, 420–479 (March–April 1983)

The experimental and theoretical studies on the structure of the Gamow–Teller β-decay strength functions are reviewed. Also considered are processes such as M1 γ decay of analog states, the emission of delayed protons, neutrons, and α particles, delayed fission, and the (p, n) reaction at proton energies 100–200 MeV. The results of measurements of the strength functions by γ-ray total absorption are analyzed. It is shown that the β^+ decay of nuclei far from the stability band exhibits a new type of collective charge-exchange excitation: Gamow–Teller resonance with $\mu_\tau = +1$.

PACS numbers: 23.40.Hc, 25.40.Ep, 23.20. – g

INTRODUCTION

The β-decay strength function S_β is one of the most important structural characteristics of a nucleus. It is the distribution with respect to the excitation energy of squares of matrix elements of β-decay type, for example, Fermi, Gamow–Teller, etc. One can speak of the distribution of the β-decay strengths averaged over some energy interval, and also without averaging. Experimental data and theoretical studies on the behavior of S_β are currently available up to an excitation energy of about 20 MeV. At low excitation energies (up to Q_β, the β-decay energy), the strength function determines the nature of the β decay of a radioactive nucleus and the half-life. At higher excitation energies not attainable in β decay, S_β determines the cross sections of various nuclear reactions that depend on matrix elements of β-decay type. Such processes are charge-exchange (p, n) reactions, $M1$ γ decay of analog resonances, and the radiative capture of mesons.

Until recently, the statistical point of view with regard to the β-decay strength functions was pre-eminent.[1] According to this point of view, β decay does not "feel" the structure of the final state, and the strength function is a smooth function of the excitation energy and can be described by the expression $S_\beta = \text{const}$ or $S_\beta \sim \rho(E)$, where $\rho(E)$ is the density of levels. This point of view was based on experimental measurements of the strength functions by the γ-ray total absorption method, but these were made with insufficient accuracy (see Sec. 3).

The first experimental data indicating a resonance nature of the strength functions were obtained from the $M1$ γ decay of analog resonances.[2-4] This was followed by experiments that contradicted the statistical interpretation: on delayed protons,[5] the (p, n) reaction,[6] delayed neutrons,[7] and direct measurements of the strength functions by γ-ray total absorption.[8-10] Discussion with the supporters of the statistical approach continued until recently.

The energy structure of S_β is determined by the isovector parts of the effective nucleon–nucleon interaction. For the analysis of resonance structure, the concept of elementary modes of nuclear excitations[11] is helpful. Charge-exchange elementary excitations, which form structure in S_β, constitute a particular class of elementary modes. They are characterized by isospin $\tau = 1$ and isospin projection $\mu_\tau = \pm 1$. In other words, these elementary excitations are not in the nuclei in which the ground state is situated but in neighboring nuclei. Ordinary elementary excitations ($\mu_\tau = 0$), for example, low-lying phonon states or giant multipole resonances, are in the same nucleus as the ground state.

From the point of view of the microscopic approach to the formation of collective states, charge-exchange excitations are a coherent superposition of particle–hole excitations of different species, for example, a proton particle and a neutron hole. The scheme of states that must be considered when analyzing the strength functions is shown in Fig. 1, while Fig. 2 gives the basic configurations that form a given collective state. The parent state with $N > Z$ (even–even) has isospin T_0 and isospin projection $T_z = T_0$. The family of particle–hole charge-exchange excitations of the type (p, n^{-1}) is situated in the neighboring nucleus whose ground state has $T = T_0 - 1$ and $T_z = T_0 - 1$. These are excitations with $\tau = 1$, $\mu_\tau = -1$. In another neighboring nucleus there may be a state with structure (n, p^{-1}).

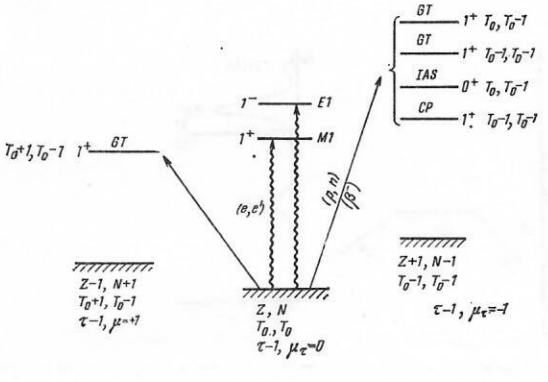

FIG. 1. States important in the analysis of β-decay strength functions: IAS, the isobar analog state; GT, Gamow–Teller resonances; CP, core-polarization states.

 0090-4759/83/020175-26$04.40

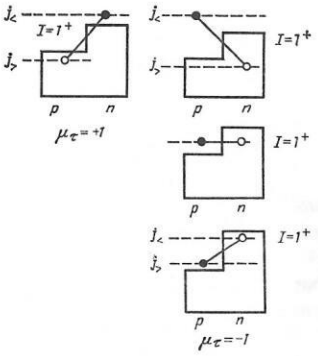

FIG. 2. The basic configurations forming charge-exchange excitations with $I^\tau = 1^+$.

This nucleus has isospin $T = T_0 + 1$ and $T_z = T_0 + 1$, and the elementary excitation has the quantum numbers $\tau = 1$, $\mu_\tau = +1$. The excitations with $\tau = 0$ and 1 and $\mu_\tau = 0$ are in the parent nucleus.

For Fermi β decay in the simple model there exists only one state, which takes the entire transition strength. This is the isobar analog state with spin 0^+, isospin $T = T_0$, $T_z = T_0 - 1$, and configuration $(p, n^{-1})_{0^+}$ (see, for example, Ref. 12). A typical strength function for Fermi decay is shown in Fig. 3.

For Gamow–Teller β transitions the situation is more complicated. A detailed analysis was made in connection with the problem of the $M1$ decay of analog resonances.[13,14,3] The main strength of the β decays is carried by the Gamow–Teller resonance $J^\tau = 1^+$, $T = T_0 - 1$, $T_z = T_0 - 1$ ($\tau = 1$, $\mu_\tau = -1$). This state has basic configuration of spin-flip type, i.e., $(p, n)^{-1}{}_{1^+}$, $j_p = l - 1/2$, $j_n = l + 1/2$, and is situated near the analog resonance. At energies lower by the spin–orbit splitting, there is a core-polarization state $J^\tau = 1^+$, $(p, n^{-1})_{1^+}$, $j_p = j_n$. At even lower energies, there are configurations of "back spin-flip" type, which are important in the analysis of β decay: $J^\tau = 1^+$, $(p, n^{-1})_{1^+}$, $j_p = l + 1/2$, $j_n = l - 1/2$. The core-polarization and back spin-flip states have normal isospin, i.e., $T = T_0 - 1$, $T_z = T_0 - 1$. Since a spin-flip configuration does not have a definite isospin, there is a $T_>(T = T_0, T_z = T_0 - 1)$ component of the Gamow–Teller resonance a few mega-electron-volts above the ground ($T_<$) resonance.

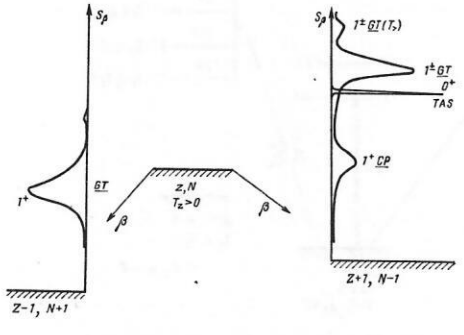

FIG. 3. Scheme of typical strength functions of Gamow–Teller β transitions. The strength function of Fermi transitions, which is concentrated in the analog state, is shown for comparison.

For β^+ decay in the simple model there is only one state $J^\tau = 1^+$, $(n, p^{-1})_{1^+}$. It has $T = T_0 + 1$, $T_z = T_0 + 1 (\tau = 1$, $\mu_\tau = +1)$ and is also called a Gamow–Teller resonance with $\mu_\tau = +1$. Its energy may vary strongly from nucleus to nucleus.

We note that from the point of view of the phenomenological approach the Gamow–Teller resonance ($\mu_\tau = -1$), $M1$ ($\mu_\tau = 0$), the giant resonance, and the Gamow–Teller resonance ($\mu_\tau = +1$) are an isobaric triplet of 1^+ states. However, from the microscopic point of view these states cannot be called isobaric triplets, since the configurations that form these states do not go over into each other under the action of the operators T_- or T_+.

The states discussed in the present paper are at high excitation energies (up to 20 MeV in heavy nuclei). At such excitation energies, the relatively simple configurations are distributed over several nuclear states with complicated structure and are manifested in different processes as a strength function[15] or intermediate structure. The widths of the resulting giant resonances depend on the strength of the interaction between the simple and the complicated configurations. From the phenomenological point of view, the existence of narrow giant resonances indicates conservation of some symmetry. Thus, the small width of the analog resonance indicates the isotopic symmetry of the nuclear interaction. The existence of the Gamow–Teller resonance can be associated with supermultiplet symmetry.[16,17] According to the available experimental data, the widths of the peaks in the β-decay strength functions are about 1 MeV at excitation energy 3–4 MeV. The widths of the Gamow–Teller resonance are 2–4 MeV. In other words, the concentration of the strength of the Fermi β transitions in the analog state leads to a strong (by three or four orders) hindrance of the β transitions between the low-lying states. The concentration of the Gamow–Teller transitions is less strong, which leads to a less strong (by one or two orders) hindrance of the transitions between the low-lying states.

The ideas about the resonance structure of the β-decay strength functions have been important in the most varied branches of nuclear physics. In traditional nuclear spectroscopy of radioactive isotopes, the logft values are sometimes used to ascribe definite configurations to levels. It is clear, however, that this can be done only after a detailed calculation of the entire strength function with allowance for all the configurations important for the given nucleus.

The spectra of delayed protons and α particles are determined both by the shape of the β-decay strength function and by the probability of proton or α decay of the populated states. Analysis of such spectra gives information about the distribution of the strength of the Gamow–Teller transitions with $\mu_\tau = +1$. From analysis of the spectra of delayed neutrons one can obtain information about the β-decay strength functions, i.e., the distribution of the strength of the Gamow–Teller transitions with $\mu_\tau = -1$. An almost uninvestigated field is the spectroscopy of delayed particles and analysis of the probabilities of emission of particles from states with Gamow–Teller-type configurations.

Delayed fission, i.e., fission after β decay, can be a unique tool for studying fission barriers for nuclei far from the stability band. However, to obtain information about a fission barrier it is necessary to make certain assumptions about the shape of the β-decay strength functions.

A topical problem is the prediction of the half-lives of nuclei far from the stability band on the basis of the structure strength function. Such data are needed for the planning of experiments with distant nuclei, for calculations of various astrophysical processes,[18] and for various technological applications.

Experimental data on the $M1$ decay of analog resonances, on the spectra of neutrons in the (p,n) reaction at high proton energies, on various charge-exchange (^{3}He, t) and (^{6}Li, ^{6}He) reactions, etc., and on reactions involving mesons give, on the one hand, information about the β-decay strength functions and, on the other, require for their interpretation well-developed ideas about the structure of the latter.

The Gamow–Teller resonance is situated in a region near the analog resonance. Both resonances can be observed as intermediate structures in proton resonances. The first experimental observation of the Gamow–Teller resonance as intermediate structure was made in the (p,γ) reaction.[19] The further investigation of charge-exchange doorway states is a new field.

The theory of Gamow–Teller-type excitations is in an initial stage of development. One can therefore hope for qualitatively new facts and ideas about nuclear structure, as usually happens when new phenomena are investigated.

1. RESONANCE NATURE OF THE β-DECAY STRENGTH FUNCTIONS

Although a resonance nature of the strength functions S_β appears perfectly natural from the physical point of view, the statistical approach, which ignores in the initial variant all structure, was widely popular. Therefore, in this section we give the main experimental facts proving the resonance nature of S_β.

Determination of S_β. The strength function S_β is found from the experimental data as follows. If the probability density $I(E)$ for population of the levels of the daughter nucleus is measured, then

$$S_\beta(E) = I(E)/[t_{1/2} f(Q_\beta - E)], \tag{1}$$

where $t_{1/2}$ is the half-life, $f(Q-E)$ is the Fermi function, and $Q_\beta - E$ is the decay energy. To this value there corresponds the theoretical value of $S_\beta(E)$:

$$S_\beta(E) = \frac{1}{D(g_V^2/g_A^2)} B'(GT, E)\,\rho(E), \tag{2}$$

where $D = 6260 \pm 60$ sec, $\rho(E)$ is the level density in the final nucleus, and

$$B'(GT, E) = \frac{1}{2I_i+1}\left\langle KI_f \left\| \sum_k t_-(k)\,\sigma_\mu(k) \right\| I_i \right\rangle = \frac{4\pi}{g_A^2} B(GT) \tag{3}$$

in the notation of Ref. 15. The distribution $B'(\mathrm{GT}, E)$, calculated by some model, makes it possible to find $S_\beta(E)$ and the half-life:

$$t_{1/2}^{-1} = \int_0^{Q_\beta} S_\beta(E)\, f(Q_\beta - E)\, dE. \tag{4}$$

If we are concerned with discrete nuclear states, then in (1) the function $I(E_i)$ is the intensity of population of level i by β decay, while $S_\beta(E_i)$ is defined differently:

$$S_\beta(E_i) = \frac{1}{D(g_V^2/g_A^2)} B'(GT, E_i). \tag{5}$$

In what follows, we shall use such a definition of S_β in the nonstatistical interpretation of the experimental data and the calculations. Until recently, virtually all experiments associated with delayed processes and all calculations of half-lives for distant nuclei[20] were analyzed with simplified assumptions about the strength function: $S_\beta = \text{const}$ or $S_\beta \sim \rho(E)$. In recent variants of the model, ideas about the Gamow–Teller resonance have been artificially included and single-particle transitions taken into account. It is now clear that it is necessary to make a detailed calculation of S_β based on a microscopic approach using the powerful modern theoretical methods for calculating giant resonances. The modern experimental data also unambiguously prove the existence of a well-developed resonance structure.

Comparison of the β^-- and β^+-Decay Strength Functions. The strength functions S_β for β^- and β^+ transitions are qualitatively different in the microscopic approach, this being manifested in the first place in the total sum of the β^+ and β^- transitions. There exists a sum rule[11] according to which the total sums S_+ and S_- satisfy

$$S_- - S_+ \approx 3\,(N - Z), \tag{6}$$

where $S_\mp = \sum_i B_\mp(\mathrm{GT}, E_i)$. This means that in nuclei with $N > Z$ the total sum of the β^- transitions is much larger than that for the β^+ transitions. However, this, naturally, does not mean that the logft values for the β^- and β^+ transitions between the low-lying states must differ strongly. Since more than 90% of the total strength of the β^- transitions is concentrated in the Gamow–Teller resonance, the strengths at low excitation energies must be comparable.

In the S_β for the β^- transitions there is always a main maximum situated in the region of the analog state. It is not so obvious that there exists a main maximum in S_β for the β^+ transitions.[21] As a rule, the collectivization of the Gamow–Teller resonance ($\mu_\tau = +1$). Evidently, the width of a main maximum in β^+ decay will be greater than the width of the Gamow–Teller resonance ($\mu_\tau = -1$). Finally, the main difference is that the excitation energy at which a main maximum in S_{β^+} is situated can vary strongly with variation in $N - Z$, whereas the maximum in S_{β^-} changes its position little. In particular, whereas the Gamow–Teller resonance ($\mu_\tau = -1$) is in principle unattainable in β decay in medium and heavy nuclei, the Gamow–Teller resonance ($\mu_\tau = +1$) may sink below Q_{β^+} in certain nuclei.[21]

At relatively low excitation energies, one must expect maxima associated mainly with single-particle transitions in the β^+ strength functions. For β^- decay, other

maxima may be observed, i.e., core-polarization states and back spin-flip states.

Despite the qualitative differences between S_β for β^+ and β^- transitions, these differences have little influence on the probabilities of β transitions between low-lying states in nuclei near the stability band. On the transition to the investigation of nuclei far from it S_β can be measured directly. In this case, manifestation of the differences is much more probable.

The $M1$ Decay of Analog Resonances. Core Polarization States.[3] The first experimental proofs of resonance structure of the strength functions S_β were obtained in the investigation of a process which at the first glance seems quite unlike β decay, namely, $M1$ γ decay of analog resonances. However, the $M1$ operator of γ decay of analog resonances ($\Delta T = 1$) is similar to the β-decay Gamow–Teller operator. Therefore, the probabilities of $M1$ decay of the corresponding analog state are related. One can obtain the following expression relating the matrix elements for the two processes:

$$\langle f|\sum_i \sigma_i \tau_-(i)|i_0\rangle = -\sqrt{2T_0}\,\langle f|\sum_i \sigma_i t_z(i)|i\rangle, \qquad (7)$$

where $|i_0\rangle$ is the parent state, $|i\rangle$ is the corresponding analog state, and $|f\rangle$ is the final state. On the left-hand side, there is the Gamow–Teller β-decay operator, and on the right the spin part of the isovector $M1$ transition. Thus, studying the strength function of $M1$ transitions from the analog, one can obtain information about the strength function of β transitions.

Since the structure of the analog is $(p n^{-1})_{0^+}$, and that of core-polarization states is $(p n^{-1})_{1^+}$, it is clear that a strong $M1$ transition must be observed between these states. Detailed analysis shows that the presence of the l part in the $M1$ operator of the γ transition enhances transitions to core-polarization states. Therefore, in the distribution of $B(M1)$ for transitions from analogs these states appear in the form of clear peaks. These states were first observed and correspondingly interpreted in Ref. 2. In Ref. 3 there is a compilation of experimental data on core-polarization states available up to 1975. In Ref. 4, it was shown that there is a linear dependence of the analog–core-polarization state distance on the isospin of the parent nucleus, which confirms the interpretation. Some typical distributions of $B(M1)$ for the decay of analogs in the region $A \approx 50$ are shown in Fig. 4. The results on the (p,n) reaction (see Sec. 8) also confirm the existence of core-polarization states. In the spectra of neutrons from the (p,n) reaction at 0° on light nuclei strong peaks situated below the analogs can be observed. These are the core-polarization states. In heavy nuclei, because of the interaction between the spin-flip configurations and the core-polarization states the strength of the transitions is transferred to the highest states (Gamow–Teller resonance), and it is difficult to observe population of the core-polarization states.

Strength Functions S_β from the Spectra of Delayed Neutrons. The discovery of core-polarization states in $M1$ decay of analogs stimulated studies on the nonstatistical interpretation of S_β obtained from the spectra of delayed neutrons. Until recently, these spectra were interpreted on the basis of the assumptions $S_\beta = \text{const}$ or $S_\beta \sim \rho(E)$. Data obtained with insufficiently good resolution admitted such an interpretation. However, the first measurements of the spectra of delayed neutrons made with high resolution[7] revealed a clear energy-dependent structure of S_β for β^- transitions. An example of the strength functions S_β for Rb isotopes obtained partly from the spectra of delayed neutrons and partly from analysis of the decay schemes of the isotopes is shown in Fig. 5. The interpretation of these strength functions on the basis of microscopic calculations is given in Ref.

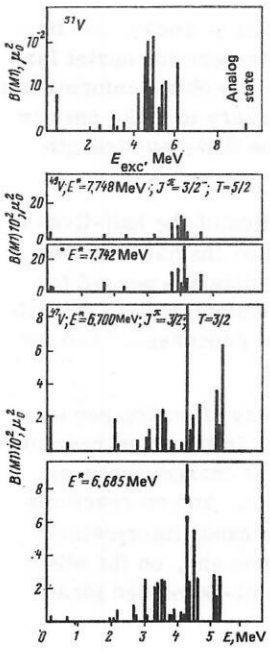

FIG. 4. Distributions of reduced probabilities $B(M1)$ for γ decay of analog states of vanadium isotopes.[3]

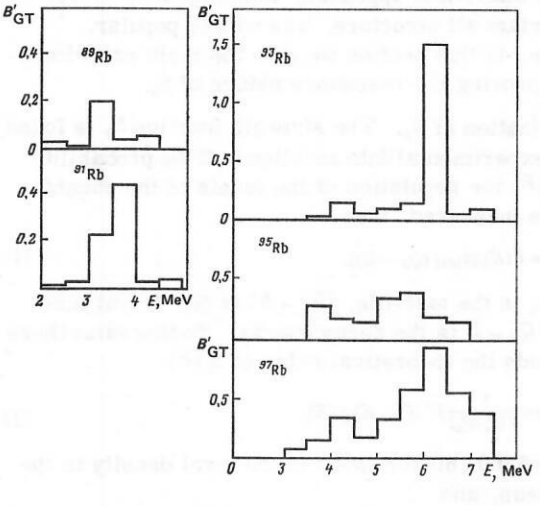

FIG. 5. Strength functions of β^- transitions for the decay of rubidium isotopes. The reduced probabilities are obtained from the experimental values of ft (Ref. 7) in accordance with Eq. (3) with allowance for the renormalization of the nuclear spin current.[5,6]

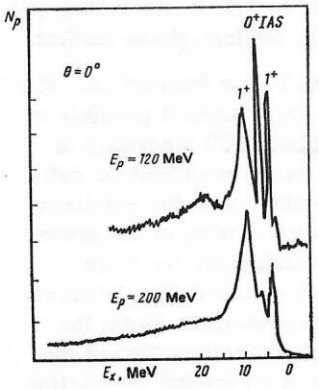

FIG. 6. Spectrum of neutrons from the $^{89}Y(p,n)$ reaction.[23]

22. We note a circumstance that, on the one hand, confirms the microscopic interpretation, and, on the other, indicates the nonrandom origin of the maxima in S_β. The position of the maxima changes in a regular manner on the transition from one nucleus to another. One actually observes the same linear dependence of the energy of the maxima, measured from the energy of the parent state, on $N-Z$ as for core-polarization states.

Gamow–Teller Resonance ($\mu_\tau = -1$) from (p,n) Reactions. At the time when the core-polarization states were discovered (1969), there was no information about the existence of the Gamow–Teller resonance. The first results appeared in 1975, when the Gamow–Teller resonance was observed in the spectrum of neutrons from the (p,n) reaction.[6] In 1980, an entire series of data from the (p,n) reaction at angle 0° and proton energies from 120 to 200 MeV was published. The first results have now been published for different nuclei from ^{26}Mg to ^{208}Pb. These data will be discussed in detail in Sec. 8. Here, we give a typical result for $^{89}Y(p,n)$ (Ref. 23) and $^{208}Pb(p,n)$ (Ref. 24) (Figs. 6 and 7). It can be seen from the figures that in the spectra of neutrons at 0° there is not only an analog state but also a Gamow–Teller resonance ($\mu_\tau = -1$) situated above it and core-polarization states. Thus, the resonance structure of S_β for β^- transitions is now reliably established on the basis of the most varied independent experiments.

Direct Measurements of S_β for β^+ Transitions. The first attempts to measure S_β by the direct method of γ-ray total absorption were made some years ago.[1] However, the parameters of the facility and the method of analysis did not correspond to the problem posed. The result obtained was that S_β is a smooth function without any maxima and is well described under statistical assumptions. These experiments were the basis for the use of the simplified ideas about S_β.

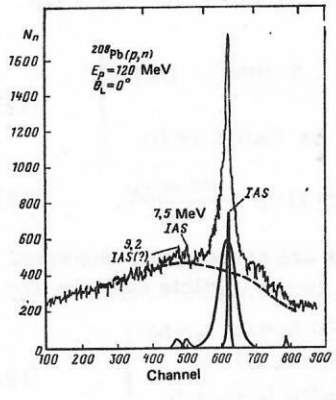

FIG. 7. Spectrum of neutrons from the $^{208}P(p,n)$ reaction.[24]

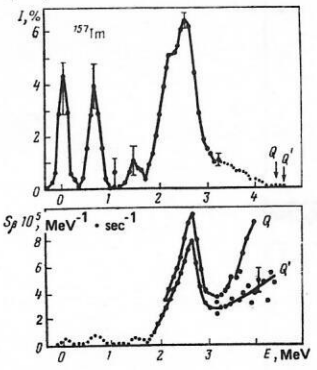

FIG. 8. Dependence of S_{β^+} for decay of ^{157}Tm on the excitation energy and on the decay energy Q (Q' is taken from the nuclear-mass systematics,[10] and Q is the limiting energy of the total-absorption spectrum).

The measurements described in Refs. 8–10 showed that the strength functions S_β for the decay of neutron-deficient nuclei have a well-defined structure (Fig. 8). The interpretation of the obtained experimental maxima must be based on sufficiently realistic calculations. It is necessary to have estimates of the positions of the maxima, the total sum, and the intensities of population of the maxima. Estimates of the position of the main maximum in S_β were made in Ref. 21. Realistic estimates of the population intensities were made in Ref. 8. Comparison of the calculated and experimental S_β made it possible to identify the Gamow–Teller resonance with $\mu_\tau = +1$.[10]

The Value of S_β from Measurement of Delayed Protons. Most measurements of the spectra of delayed protons give a smooth strength function S_β after analysis.[5] However, there are data which definitely indicate the existence of a maximum in S_β. One of the first cases is ^{109}Te. Figure 9 shows S_β for ^{114}Cs.[25]

Since it is possible to obtain from the spectra of delayed protons information about S_β only in a narrow interval of excitation energies, the identification of the main maximum must be based on comparison with reliable theoretical calculations. Calculations that we have made enable us to assert that for ^{114}Cs a main maximum is observed in S_β.

2. THEORETICAL DESCRIPTION OF THE β-DECAY STRENGTH FUNCTIONS

The problem of the microscopic description of the β-decay strength functions is intimately related to problems of the theoretical analysis of $\log ft$ for β transitions between low-lying states, $M1$ γ decay of analogs, and the properties of the Gamow–Teller resonance.

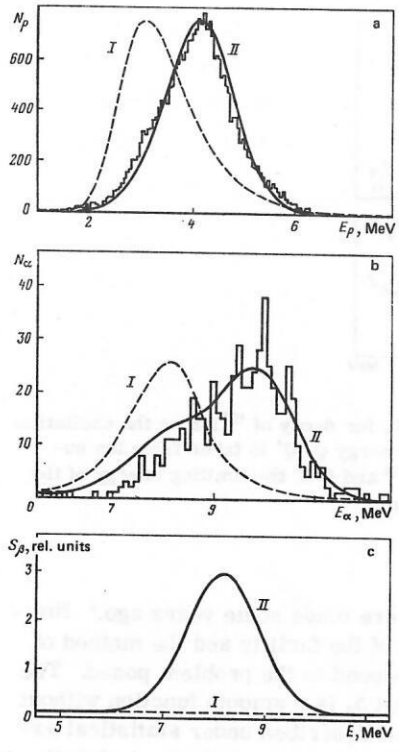

FIG. 9. Energy dependence of S_{β^+} for ^{114}Cs obtained in Ref. 25 by analyzing the spectra of delayed protons and α particles.

It is known that Gamow–Teller β transitions between low-lying states are hindered compared with the single-particle estimate. Allowance for pair correlations improves the agreement between the theoretical and experimental values of logft.[26] Calculations of the probabilities of β transitions based on ideas about collective charge-exchange excitations were first made in Ref. 27. Equations of the random-phase method were obtained for charge-exchange excitations for spherical[28] and deformed[29] nuclei. Systematic investigations of the Gamow–Teller resonance and other collective states were made in Refs. 17 and 30. The position of the Gamow–Teller resonance with allowance for one-pion exchange was calculated in Ref. 31.

A schematic model taking into account the isospin–isospin and spin–isospin residual interaction[14] was used to calculate the strength functions S_β for a large number of nuclei. The model was originally used to analyze $M1$ decay of analog resonances,[14,4,32] the strength functions of β transitions from spectra of delayed neutrons,[22] and the intensity of delayed fission.[33] In all cases, S_β was calculated for β transitions: for the Cu, Sc, and V isotopes in Refs. 14 and 4, for the As isotopes in Ref. 32, for Rb in Ref. 22, and for Pa in Ref. 33. In Ref. 86, S_β were calculated for many nuclei with $A=250$–266, $N=165$–175. In all these cases, the positions and population intensity of the Gamow–Teller resonance were calculated. In Refs. 8 and 21, the model was used to calculate S_β for β decay and the position of the Gamow–Teller resonance with $\mu_\tau=+1$ in connection with experimental data on S_β from the decay of neutron-deficient isotopes. In Ref. 9, the model was generalized in the spirit of the random-phase method.

Role of the Residual Gamow–Teller Interaction. The introduction of the isospin concept made it possible to explain the very strong (by about $\sim 10^4$) hindrance of 0^+–0^+ Fermi β transitions in nuclei with neutron deficiency. This effect was associated with the existence of a collective state—the isotopic analog of the ground state of the parent nucleus, which takes the main strength of the Fermi β transitions and is situated above the ground state of the decaying nucleus. From the microscopic point of view, the collectivization of the analog is due to the existence of a residual interaction of the form

$$V_{\tau\tau}=G_{\tau\tau}(\tau_1\tau_2), \tag{8}$$

which restores the charge symmetry broken at the microscopic level.

The matrix elements of Gamow–Teller β transitions to low-lying states are also hindered by 10–100 times compared with the single-particle estimates. Just as the hindrance of the Fermi transitions [the operator $\beta_F^\pm=\sum_k\tau_\pm(k)$] can be explained by taking into account a residual interaction of the type (8), to explain the hindrance of the Gamow–Teller transitions [the operator $\beta_{GT}^\pm=\sum_k\tau_\pm(k)\sigma(k)$] a residual interaction of the following form was introduced in Ref. 27:

$$V_{\tau\tau\sigma\sigma}=G_{\tau\sigma}(\tau_1\tau_2)(\sigma_1\sigma_2). \tag{9}$$

Model for Calculation of the Strength Functions. The Hamiltonian of the system can be represented as a sum of a single-particle part and the charge-exchange residual interactions (8) and (9):

$$H=H_{SP}+V_{\tau\tau}+V_{\tau\tau\sigma\sigma}. \tag{10}$$

As basis functions, one takes the states obtained from the parent state $|\Psi_0\rangle$ by applying the β-decay operator; then the matrix elements of the Gamow–Teller interaction (9) are represented in the factorized form

$$\langle f|V_{\tau\tau\sigma\sigma}|f'\rangle=G_{\tau\sigma}V_fV_{f'}, \tag{11}$$

where the V_f are proportional to the amplitudes of the β transitions to the corresponding states $|f\rangle$ of the chosen basis.

In particular, for the β decay of a Z-odd nucleus the basis states include single-particle neutron states and three-particle states of the type $p_0(pn^{-1})_{1^+}$ with $I=j_{p_0}$, $j_{p_0}\pm1$:

$$\left.\begin{aligned} V_{j_{n_0}}&=\frac{v_{j_{p_0}}v_{j_{n_0}}}{\sqrt{2j_{n_0}+1}}\langle j_{n_0}\|\sigma\|j_{p_0}\rangle \quad \text{for states} \quad |j_{n_0}\rangle;\\ V_{j_{p_0}j_pj_n}&=\frac{u_{j_p}u_{j_n}}{\sqrt{3}}\langle j_p\|\sigma\|j_n\rangle \quad \text{for} \quad |j_{p_0}(j_pj_n)_1+I\rangle; \end{aligned}\right\} \tag{12}$$

$$B'_{GT}=\frac{2I_f+1}{2j_{p_0}+1}V_f^2;\quad ft=\frac{6260\,(g_V^2/g_A^2)}{B'_{GT}}. \tag{13}$$

For β^- decay, the energies are conveniently measured from the analog. Then the single-particle energies are

$$\left.\begin{aligned} &E_{j_{n_0}}=E_{j_{p_0}(j_pj_n)_{1^+}}=-2G_{\tau\tau}T_0;\ j_{p_0}=j_{n_0};\ j_p=j_n;\\ &E_{j_{n_0}}=-2G_{\tau\tau}T_0\pm E_{ls}(p_0);\ j_{n_0}=j_{p_0}\pm1;\\ &E_{j_{p_0}[(j_pj_n)_{1^+}]_I}=-2G_{\tau\tau}T_0\pm E_{ls}(p);\ j_n=j_p\pm1, \end{aligned}\right\} \tag{14}$$

TABLE I. Wave functions of ^{135}Te states for $I^\pi = 7/2^+$.

E, MeV	I^π	State						B_{GT}
		CP	1	2	3	4	5	
14.3	7/2+	0.54	0.47	0.30	0.55	0.19	0.23	33.22
3.6	7/2+	0.10	0.65	0.10	−0.74	0.10	0.03	0.08
2.6	7/2+	0.14	−0.41	0.21	−0.20	0.84	0.04	0.08
2.1	7/2+	0.26	−0.34	0.74	−0.22	−0.46	0.07	0.19
0.9	7/2+	0.74	−0.25	−0.55	−0.20	−0.16	0.14	0.39
−1.8	7/2+	−0.26	−0.06	−0.06	−0.05	−0.03	−0.96	0.11

Note. The ^{135}Te configurations:

CP − $|g_{7/2}\,p\,(d_{5/2}\,p\,d_{5/2}\,n)_{1^+}\,I>$
$|g_{7/2}\,p\,(g_{7/2}\,p\,g_{7/2}\,n)_{1^+}\,I>$
$|g_{7/2}\,p\,(s_{1/2}\,p\,s_{1/2}\,n)_{1^+}\,I>$
$|g_{7/2}\,p\,(d_{3/2}\,p\,d_{3/2}\,n)_{1^+}\,I>$
$|g_{7/2}\,p\,(h_{11/2}\,p\,h_{11/2}\,n)_{1^+}\,I>$
$|g_{7/2}\,p\,(f_{7/2}\,p\,f_{7/2}\,n)_{1^+}\,I>$

1 − $|g_{7/2}\,p\,(g_{7/2}\,p\,g_{9/2}\,n)_{1^+}\,I>$
2 − $|g_{7/2}\,p\,(d_{3/2}\,p\,d_{5/2}\,n)_{1^+}\,I>$
3 − $|g_{7/2}\,p\,(h_{9/2}\,p\,h_{11/2}\,n)_{1^+}\,I>$
4 − $|g_{7/2}\,p\,(f_{5/2}\,p\,f_{7/2}\,n)_{1^+}\,I>$
5 − $|g_{7/2}\,p\,(d_{5/2}\,p\,d_{3/2}\,n)_{1^+}\,I>$

where E_{ls} is the energy of the spin–orbit splitting, which one can choose, for example, in the form $E_{ls} = (10-14)(2l+1)/A^{2/3}$. Since the excitation energy in β^- decay is fairly high, the influence of the pair correlations can be ignored.

Diagonalization of the matrix $H_{ff'} = E_f\delta_{ff'} + G_{\tau\alpha}V_fV_{f'}$ gives the energies and wave functions of the states of the daughter nucleus and makes it possible to determine the transition probability B'_{GT}. As an example, we give the results of calculations of the strength functions for decay of Te isotopes. In Table I, we give the wave functions for the decay of ^{135}Te.

Theoretical Description of the Strength Functions of β^+ Decay. There is a fundamental difference between the general nature of the β^+ and β^- strength functions, namely, in the latter the principal maxima are situated in the region of the analog, i.e., about $\Delta\mathscr{E}_{Coul}$ above the ground state of the decaying nucleus, while in former the position of the maximum cannot be related to the position of the analog, since in nulcei with $T_z > 0$ there is no analog state with respect to β^+ decay.

In order to find the energy position of the main maximum of the strength function for various nuclei and estimate the regions of nuclei for which this maximum is accessible to study in the β^+ decay of neutron-deficient nuclei far from the stability band, calculations were made of the β^+ strength functions of even–even and odd nuclei in the framework of the model[21] described above. We mention some features in the calculation of the β^+ decay strength functions. The main difference from β^- decay is that the excitation energies of the states are measured from the ground state of the daughter nucleus, and the results of the calculations for β^+ decay are more sensitive to the choice of the average field. It is found that in some nuclei the maximum in the strength function is situated at comparatively low energies, at 2–3 MeV, and therefore the influence of pair correlations on its position is important. To simplify the calculations, it was assumed in Ref. 21 that in odd nuclei the three-particle excitations are separated from the single-particle excitations by a gap of width Δ, and this parameter was varied in the calculations. Such an assumption is entirely justified in a schematic model, since the correct allowance for pairing effects in charge-exchange excitations is a very complicated problem.

For β^+ decay, the expressions (12) and (13) take the form

$$V_f = \frac{\zeta_{pn}}{\sqrt{2I_f+1}}\langle n\|\sigma\|p\rangle,$$

where $\zeta_{pn} = v_pu_n$, $E_f = E_p + E_n + \Delta$ for decay of even–even nuclei and for transitions to three-particle states in odd nuclei, $\zeta_{pn} = v_pv_n$, $E_f = E_{p0}$ for single-particle transitions in the decay of N-odd nuclei, and $\zeta_{pn} = u_pu_n$, $E_f = E_{n_0}$ for single-particle transitions in the decay of Z-odd nuclei; $B'_{GT} = (2I_f+1)V_f^2/(2I_i+1)$, where I_i is the spin of the parent nucleus, and I_f is the spin of the final states, $I_f = I_i$, $I_i \pm 1$, $I_f > 0$.

The residual interaction leads to mixing of the states, to redistribution of the transition strength, and to a shift of the excitation energy of the states. The energies and transition probabilities are obtained by diagonalizing the matrix (12). The results of calculations for odd A are given in Table II. Nuclei with $T_z > 0$ and $B_p > 0$ were considered.

1. Nuclei of the $f_{7/2}$ shell, $22 \leq Z \leq 28$. In the β^+ decay of all nuclei of this region, the main maximum of the strength function is above the ground state of the parent nucleus. As the $f_{7/2}$ shell is filled with both protons and neutrons, the energy of the maximum sinks.

2. Nuclei of the f–p shell, $29 \leq Z \leq 38$. For $Z \leq 32$, the ground state of the Z-odd nuclei is $p_{3/2}$. For N-odd nuclei, the configurations $f_{5/2}$ and $p_{3/2}$ are possible. In the absence of experimental data, the calculations were made for two possible spins of the ground states. The position of the maximum is not very sensitive to the chosen value. In all cases, the maximum lies above Q and cannot be populated by β decay.

For nuclei with $Z = 33-38$, it was assumed that the level $p_{1/2}$ is populated after the level $g_{9/2}$. The calculations were made under the assumption that the ground states are characterized by the configurations $p_{3/2}$ or $f_{5/2}$ for $N \leq 38$ and $p_{1/2}$ or $g_{9/2}$ for $N > 38$. In the decay of the light Br, Sr, Rb isotopes a main maximum of the strength function can be observed. In Table II, we give data for the $9/2^+$ ground or isomer states.

3. Nuclei of the $g_{9/2}$ shell. In the calculations, it was assumed that the level $p_{1/2}$ is populated after the level $g_{9/2}$. The neutron levels $d_{5/2}$ and $g_{7/2}$ were assumed to be degenerate. For N and $Z < 50$, the calculations were made for two spin values of the parent states. In Table II, we give the values for $I_i^\pi = 9/2^+$. For nuclei with $N < 50$, the strength functions have two maxima: a local one with energy around 3 MeV and the main one at $E \approx 7$ MeV. For $N > 50$, the main maximum is at a low excitation energy.

4. Nuclei of the $g_{7/2}$–$d_{5/2}$ shell, $51 \leq Z \leq 64$. For $N < 64$, the strength functions have two maxima, a local one with energy 3 MeV associated with the $d_{5/2}$–$d_{3/2}$ transition, and the main one with energy around 5 MeV associated with the transition $g_{9/2} - g_{7/2}$. For $N > 64$, the maximum associated with the transition $g_{9/2} - g_{7/2}$

TABLE II. Position of the main maximum in the β^+-decay strength functions.[21]

Nuclide	E, MeV	Nuclide	E, MeV	Nuclide	E, MeV
$^{22}Ti^{23}$	7.7	Mo^{47}	7.3	Te^{65}	2.6
$^{23}V^{24}$	8.2	Mo^{49}	7.3	$^{53}I^{56}$	6.0
$^{24}Cr^{25}$	8.4	$^{43}Tc^{44}$	7.5*	I^{58}	5.7
$^{25}Mn^{26}$	7.3	Tc^{46}	7.5*	I^{60}	5.3
$^{26}Fe^{27}$	8.9	Tc^{48}	7.5	I^{62}	4.9
$^{27}Co^{28}$	4.1	Tc^{50}	2.0*	I^{64}	2.7
Co^{30}	4.0	$^{44}Ru^{45}$	8.1*	I^{66}	1.2*
$^{28}Ni^{29}$	3.6	Ru^{47}	8.0	$^{55}Xe^{57}$	5.9*
$^{29}Cu^{30}$	9.0	Ru^{49}	7.5	Xe^{59}	5.5*
Cu^{32}	8.1	Ru^{51}	1.8*	Xe^{61}	5.1*
$^{30}Zn^{31}$	8.2	$^{45}Rh^{46}$	8.3*	Xe^{63}	4.8*
Zn^{33}	7.6	Rh^{48}	8.1*	Xe^{65}	2.7*
Zn^{35}	7.1	Rh^{50}	2.3*	Xe^{67}	1.2*
$^{31}Ga^{32}$	8.0	Rh^{52}	2.0*	$^{55}Cs^{58}$	6.0*
Ga^{34}	7.1	Rh^{54}	1.7*	Cs^{60}	5.4*
$^{32}Ge^{33}$	7.7	$^{46}Pd^{47}$	7.8*	Cs^{62}	5.0*
Ge^{35}	7.3	Pd^{49}	7.4*	Cs^{64}	2.9*
$^{33}As^{34}$	6.8	Pd^{51}	2.6*	Cs^{66*}	1.4*
As^{36}	6.0	Pd^{53}	2.2*	$^{56}Ba^{59}$	5.6*
As^{38}	2.3	$^{47}Ag^{48}$	8.4*	Ba^{61}	5.2*
$^{34}Se^{35}$	8.2	Ag^{50}	2.5*	Ba^{63}	4.9*
Se^{37}	6.4	Ag^{52}	2.2*	Ba^{65}	2.8*
Se^{39}	2.6	Ag^{54}	1.9*	Ba^{67} [1]	1.3*
$^{35}Br^{36}$	6.4*	Ag^{56}	1.8*	$^{57}La^{62}$	5.0*
Br^{38}	3.2*	$^{48}Cd^{49}$	8.0*	La^{64}	2.9*
Br^{40}	2.3*	Cd^{51}	3.0*	La^{66} [1]	1.5*
$^{36}Kr^{37}$	7.5	Cd^{53}	2.6*	$^{58}Ce^{63}$	4.8*
Kr^{39}	3.0*	Cd^{55}	2.2	Ce^{65} [1]	1.5*
$^{37}Rb^{38}$	2.3*	Cd^{57}	2.0	$^{59}Pr^{64}$	1.8*
Rb^{40}	2.3*	$^{49}In^{50}$	3.3	Pr^{66} [1]	1.7*
Rb^{42}	2.3*	In^{52}	3.0	$^{60}Nd^{67}$ [1]	1.6*
Rb^{44}	2.3	In^{54}	2.5	Nd^{69} [2]	1.5*
$^{38}Sr^{39}$	2.7*	In^{56}	2.3	$^{61}Pm^{66}$ [2]	1.8*
Sr^{41}	2.6*	In^{58}	2.0	$^{62}Sm^{69}$ [2]	1.7*
Sr^{43}	2.4*	In^{60}	1.6	$^{63}Eu^{68}$ [2]	1.8*
Sr^{45}	2.3	$^{50}Sn^{53}$	2.5	$^{64}Gd^{71}$ [2]	1.7*
$^{39}Y^{40}$	5.3*	Sn^{55}	2.2	$^{65}Tb^{74}$	6.0*
Y^{42}	5.3*	Sn^{57}	2.0	Tb^{76}	6.0*
Y^{44}	5.3	Sn^{59}	1.8	Tb^{78}	6.0*
Y^{46}	5.3	$^{51}Sb^{52}$	6.8	Tb^{82} [3]	2.0*
$^{40}Zr^{41}$	6.4*	Sb^{54}	6.3	$^{66}Dy^{73}$	7.4*
Zr^{43}	6.4*	Sb^{56}	6.0	Dy^{75}	7.4*
Zr^{45}	6.5	Sb^{58}	5.7	Dy^{77}	7.4*
Zr^{47}	6.5	Sb^{60}	5.3	Dy^{79}	7.4*
$^{41}Nb^{42}$	7.0*	Sb^{62}	4.9	Dy^{81}	7.4*
Nb^{44}	7.0*	$^{52}Te^{55}$	6.2	Dy^{83} [3]	1.4*
Nb^{46}	7.0	Te^{57}	5.9	$^{67}Ho^{76}$	7.6*
Nb^{48}	7.0	Te^{59}	5.5	Tm^{82} [3]	3.0*
$^{42}Mo^{43}$	7.4*	Te^{61}	5.1	$^{70}Yb^{81}$	7.7*
Mo^{45}	7.3*	Te^{63}	4.8	Yb^{83} [3]	2.7*
Ho^{78}	7.6*	Er^{81}	7.8*		
Ho^{80}	7.6*	Er^{83} [3]	2.7*		
Ho^{82} [3]	2.5*	$^{69}Tm^{78}$	7.9*		
$^{68}Er^{79}$	7.8*	Tm^{80}	7.9*		

Notes. With further increase in N to the point at which the stability line is left, the energy of the maximum remains in the interval 1–1.5 MeV. 2. With further increase in N up to $N = 80$, the energy of the maximum remains in the range 1–1.5 MeV. 3. For the decay of nuclei with $N \geq 82$, the energy of the maximum remains in the range 1.5–2.5 MeV. *The maximum is situated below Q and can be populated by β^+ decay.

disappears, and the first maximum sinks to energies 1–2 MeV.

5. Nuclei of the $h_{11/2}$ shell, $65 \leq Z \leq 70$, are deformed for $N > 90$. For the lighter isotopes, the calculation in the spherical limit is valid. In the calculation, it was assumed that the neutron $s_{1/2}, d_{3/2}, h_{11/2}$ states are degenerate. For the majority of the isotopes, the main maximum lies below Q. For the lightest isotopes, it is at height 6–8 MeV. For $N > 82$, the main maximum of the strength function is at energy 2–3 MeV.

6. Nuclei with $Z = 71$–81. The position of the main maximum depends weakly on N and Z. For nuclei with $Z = 71$–76, the excitation energy is 2–3 MeV; for nuclei with $Z = 77$–78, the maximum is at 1–2 MeV.

As the results of these calculations show, the strength functions of β^+ and β^- decay are qualitatively different. In the former, the position of the maximum and, therefore, the shape of the strength function can vary strongly from nucleus to nucleus. The degree of collectivization of the resonance increases with decreasing A and T_z, though in the lightest nuclei with $T_z > 0$ the maximum is evidently above the ground state of the parent nucleus. For many neutron-deficient isotopes in the region $35 < Z$ this maximum can be populated in β^+ decay.

Influence of Deformation on the β-Decay Strength Functions. From the macroscopic point of view, the collective Gamow–Teller excitations are oscillations of the spin–isospin density without change in the shape of the nucleus, and therefore the position of the maximum in the spherical limit must correspond approximately to the centroid of the strength function of the deformed nucleus. A generalization of the model described above for deformed nuclei was given in Ref. 8 for the description of the β^+-decay strength functions of Lu isotopes. In β^+ decay, a significant contribution to the strength function is made by transitions between states near the Fermi surface, so that for deformed nuclei it is necessary to take into account pair correlations. Detailed expressions for the decay of odd–odd nuclei are given in Ref. 8.

The results of calculations for the decay of ^{165}Lu are given in Fig. 10 and in Table III. From comparison with the experimental data obtained by the total-absorption method[8] it can be seen that the calculations reproduce well the positions and relative intensities of the maxima, although the absolute values of the transition probabilities are almost an order of magnitude too high. One of the reasons for this is the neglect of the correlations in the ground state associated with the interaction of charge-exchange modes with $\mu_\tau = \pm 1$ in the method used in these studies. Correlations in the ground state can be taken into account by using the random-phase approximation (RPA).

Solutions of the RPA equations for the odd Tm isotopes were obtained in Ref. 10. The calculations were made in the deformed Woods–Saxon potential, and the coupling constant was $G_{\tau\sigma} = 50/A$. In Fig. 11, we compare the results of the calculation with the experimental data obtained by the total-absorption method.[10] From comparison of the experimental and calculated data it can be seen that allowance for the correlations in the ground state by the RPA makes it possible to obtain absolute values of S_β near the experimental values. The calculations took into account the meson renormalization of

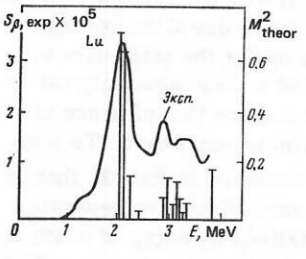

FIG. 10. Energy dependence of S_{β^+} for ^{165}Lu decay obtained in Ref. 8 by γ-ray total absorption.

TABLE III. The β^+-decay strength function of ^{165}Lu.[8]

K	E	B	Configuration
5/2	2,06	0.75	$p_0 404\downarrow - p_0 523\uparrow + n 523\downarrow$
9/2	2,06	0.75	$p_0 404\downarrow + p_0 523\uparrow - n 523\downarrow$
5/2	2.90	0.11	$p_0 404\downarrow - p_0 523\uparrow + n 512\uparrow$
9/2	2,90	0.11	$p_0 404\downarrow + p_0 523\uparrow - n 512\uparrow$
5/2	3,10	0.05	$p_0 404\downarrow - p_0 532\uparrow + n 521\uparrow$
9/2	3,10	0.05	$p_0 404\downarrow + p_0 532\uparrow - n 521\uparrow$
7/2	3,16	0.18	$p_0 404\downarrow + p_0 532\uparrow - n 523\downarrow$
7/2	3.78	0.26	$p_0 404\downarrow + p_0 523\uparrow - n 514\downarrow$
7/2	4,10	0.04	$p_0 404\downarrow + p_0 541\uparrow - n 521\uparrow$
7/2	4,18	0.04	$p_0 404\downarrow + p_0 532\uparrow - n 512\uparrow$
5/2	4.21	0.24	$p_0 404\downarrow + p_0 541\uparrow - n 523\downarrow$
9/2	4.21	0.24	$p_0 404\downarrow - p_0 541\uparrow + n 523\downarrow$
5/2	4.77	0.05	$p_0 404\downarrow - p_0 514\uparrow + n 514\downarrow$
9/2	4.77	0.05	$p_0 404\downarrow + p_0 514\uparrow - n 514\downarrow$
5/2	4.86	0.01	$p_0 404\downarrow + p_0 532\uparrow - n 514\downarrow$
9/2	4.86	0.01	$p_0 404\downarrow - p_0 532\uparrow + n 514\downarrow$
5/2	4,94	0.20	$p_0 404\downarrow - p_0 541\uparrow + n 521\downarrow$
9/2	4.94	0.20	$p_0 404\downarrow + p_0 541\uparrow - n 521\downarrow$
5/2	5.50	0.25	$p_0 404\downarrow - p_0 550\uparrow - n 521\downarrow$
7/2	5.50	0.13	$p_0 404\downarrow + p_0 550\uparrow - n 521\downarrow$
9/2	5.50	0.25	$p_0 404\downarrow + p_0 550\uparrow + n 521\downarrow$
5/2	6.96	0.22	$p_0 404\downarrow - p_0 541\uparrow + n 530\uparrow$
9/2	6.96	0.22	$p_0 404\downarrow + p_0 541\uparrow - n 530\uparrow$
7/2	7.40	0.16	$p_0 404\downarrow + p_0 541\uparrow - n 512\downarrow$

the nuclear spin current on the basis of the results of Ref. 56. This renormalization leads to a decrease in the transition probabilities by 3.1 times. It follows from the results of the calculations that in the Tm isotopes with $A \leq 159$ more than 80% of the total strength of the β^+ transitions is concentrated on the interval of excitation energies from 0 to Q. Therefore, in this case there is population by β decay of the Gamow–Teller resonance with $\mu_\tau = +1$.

3. EXPERIMENTAL INVESTIGATION OF THE β-DECAY STRENGTH FUNCTIONS BY THE TOTAL-ABSORPTION METHOD

For nuclei near the stability band the probabilities of population of levels of the daughter nucleus in β decay can be obtained from a balance of the decay schemes, though from the point of view of studying the strength functions the most interesting case is the decay of nuclides with large decay energy Q, i.e., those furthest from the stability band. The traditional spectroscopic methods are based on the use of spectrometers with high resolution and low efficiency and, therefore, require sources of high intensity and a long measurement time. With increasing decay energy, the number of transitions increases catastrophically, and for nuclides with $Q \approx 4$–5 MeV when $A > 100$ only 20–50% of the total β-decay intensity is concentrated in decay schemes containing hundreds of transitions. Therefore, the data on S_β obtained by balancing such decay schemes are not very reliable.

A method of direct measurement of the level population probabilities in β decay was proposed in Refs. 37–40. The principle of this method is that the γ rays accompanying the decay are detected by a large NaI crystal in a nearly 4π geometry. If the efficiency of total absorption of the γ rays is sufficiently high, the pulse height in such a spectrometer is determined by the total energy of the γ rays in the case, i.e., by the energy of the level populated by the β transition. At the same time, special measures must be taken to shield the crystals from β particles entering them.

In the spectrometers considered in Refs. 37–40, the source was placed between two NaI crystals, the signals from these being added. To eliminate distortions due to β particles entering the crystals, coincidences with electrons emitted in the gap between the crystals were used in Ref. 37, in which the β^--decay strength functions were measured, while in the measurement of the β^+ strength functions in Ref. 38 the crystals were shielded by a thin (approximately 2.5 mm) layer of scintillation plastic, whose signals were sent to an anticoincidence circuit, i.e., the strength functions of ε capture were measured. The need for such shielding meant that 4π solid angle could not be obtained. For these spectrometers, the solid angle was 80% of 4π, and the efficiency of the total absorption of the energy of the γ-ray cascade depended rather strongly on the number of γ rays in the cascade, i.e., on the decay scheme of the excited states (Fig. 12). Therefore, to obtain S_β by analyzing the experimental spectra the decay schemes were simulated by the Monte Carlo method,[40] and it was assumed that both the β decay and the γ de-excitation of the levels are statistical in nature. The obtained β^+ and β^- strength functions are shown in Figs. 13 and 14. Plotted on a logarithmic scale, they do indeed have a monotonic nature—if there is population of individual groups of levels, then it is manifested only in a certain "sinuosity" of the obtained curves. These data were usually quoted as direct confirmation of the statistical model of β decay. However, the assumption of a statistical nature of the decay was fed into the method of analysis *a priori*. The uncertainty of the obtained results may be very large. We note that the paper does not even give an estimate of the experimental errors for the strength functions.

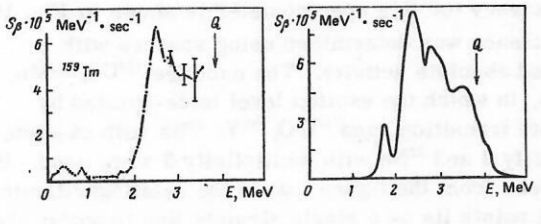

FIG. 11. Energy dependence of S_{β^+} for ^{159}Tm decay. Experiment and calculation from Ref. 10.

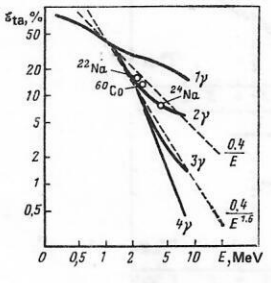

FIG. 12. Efficiencies of total absorption of the cascade of γ transitions for the spectrometer used at CERN.[39]

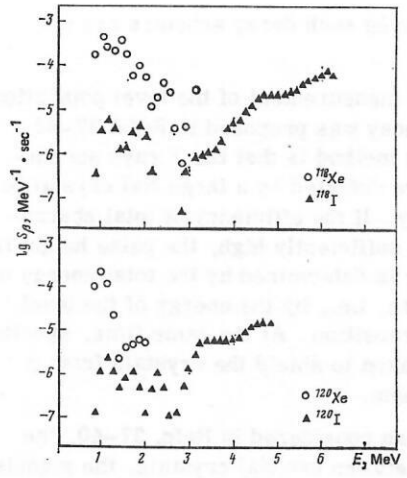

FIG. 13. Strength functions of β^+ decay.[38]

In view of the fundamental importance of direct measurements of the β-decay strength functions, conditions were formulated in Ref. 41 under which a total-absorption spectrometer can be used to obtain β-decay strength functions in a wide range of excitation energies. We give the main results of Ref. 41.

To characterize the scintillation and semiconductor γ-ray spectrometers one usually introduces the concept of the photoefficiency ε_{ph}, i.e., the ratio of the number of pulses in the total-absorption peak to the number of γ rays incident on the crystal. The principle of operation of a total-absorption spectrometer is based on summation of the energies of the cascade γ rays in a near-4π geometry. The resolving time of the spectrometer is about 1 μsec, which is much longer than the lifetime of nuclear levels. The main parameter that characterizes the operation of such a spectrometer is not the photoefficiency, but the ratio of the number of pulses in the total-absorption peak to the number of β transitions that populate this level. We shall call this quantity the cascade total-absorption efficiency, ε_{ta}, and formulate conditions under which it does not depend on the de-excitation scheme of the excited states, i.e., does not depend on the number of γ rays in the cascade or on their energies.

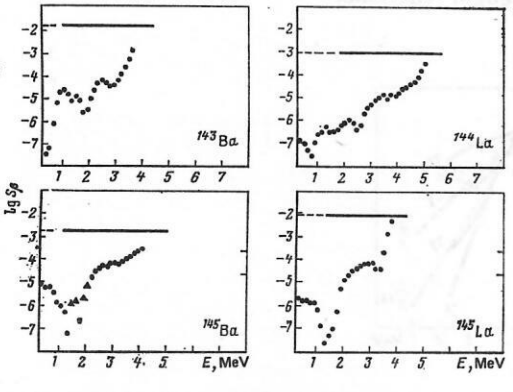

FIG. 14. Strength functions of β^- decay.[37]

If $\varepsilon_{ta} = 1$, then, irrespective of the method of de-excitation of the excited states, the experimental spectrum is the probability density for excitation of the levels of the daughter nucleus and one does not require any further analysis apart from the introduction of corrections for the finite energy resolution of the instrument. It follows from $\varepsilon_{ta} = 1$ that $\varepsilon_{ph} = 1$, and the solid angle is $\Omega = 4\pi$. For NaI crystals of the available sizes, the condition $\varepsilon_{ph} \approx 1$ is satisfied only for energies of several hundred kilo-electron-volts. At high energies $\varepsilon_{ph} < 1$, and ε_{ta} may depend on the de-excitation scheme of the levels. If ε_{ta} is to be independent of the number of γ rays in the cascade, we require $\Omega = 4\pi$ and ε_{ph} satisfying the functional equation

$$\varepsilon_{ph}\left(\sum_{i=1}^{N} E_i\right) = \prod_{i=1}^{N} \varepsilon_{ph}(E_i), \tag{15}$$

where E_i are the energies of the γ rays in the cascade and N is the number of transitions in the cascade. This equation has the solution

$$\varepsilon_{ph}(E) = \exp(-\alpha E). \tag{16}$$

Then for ε_{ta} we have

$$\varepsilon_{ta}(E) = (\Omega/4\pi)^N \exp(-\alpha E). \tag{17}$$

If $\Omega < 4\pi$, then even when the condition (16) is satisfied there is a still a strong dependence on the multiplicity of the cascade.

With increasing energy of the excited level, the transition energies increase, and the probability of detecting the γ rays decreases. This effect can be characterized by the parameter ε_t, which is equal to the ratio of the number of detected pulses to the total number of β transitions that populate the corresponding level of the daughter nucleus, i.e., ε_t is the total efficiency of the spectrometer.

On the basis of the above analysis, a total-absorption spectrometer was constructed[41] that made it possible to measure the probabilities of level population by β decay in a wide range of excitation energies. This spectrometer used one main NaI crystal measuring $\phi 200 \times 200$ mm with a pit measuring $\phi 40 \times 100$ mm, in which the source was placed, and two additional crystals measuring $\phi 200 \times 100$ mm, used to increase the efficiency. For operation with a mass separator a conveyor belt is used to transport the activity. Within the pit a thin Si(Li) detector is placed, which makes it possible to measure the total-absorption spectra in coincidence with positrons. To prevent β particles entering the NaI crystal, the source is surrounded by a plastic absorber (Fig. 15). The dependence of the cascade total-absorption efficiency for this spectrometer is shown in Fig. 16. The efficiency was determined using sources with calibrated absolute activity. The nuclides ^{137}Cs, ^{54}Mn, and ^{65}Zn, in which the excited level is de-excited by one direct transition, and ^{60}CO, ^{88}Y, ^{24}Na with cascade multiplicity 2 and ^{22}Na with multiplicity 3 were used. It can be seen from the figure that in the semilogarithmic scale all points lie on a single straight line to within the experimental errors, i.e., ε_{ta} does not depend on the number of transitions in the cascade. In the lower part

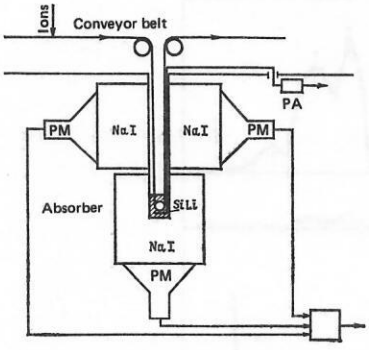

FIG. 15. Total-absorption spectrometer ensuring solid angle $\Omega = 4\pi$. An SI(Li) detector is sued to detect the β particles; PA is a preamplifier; PM is a photomultiplier; Σ is an integrating amplifier.[41]

of the figure we give the dependence of ε_t on the energy for direct transitions. For cascade transitions, ε_t is defined as the sum of the probabilities of independent events and, therefore, even for $N = 2$ is effectively 100%. For comparison, in Fig. 12 we show the energy dependence of ε_{ta} for a spectrometer without a pit[37,38] obtained by numerical simulation by the Monte Carlo method.[40] It can be seen from the figure that the violation of the condition (16) leads to a very strong dependence of ε_{ta} on the cascade multiplicity.

Method of Analyzing Total-Absorption Spectra. Let $\mathscr{E}_m$ be the energy of the m-th level populated in β decay with probability $F(\mathscr{E}_m)$. Then the count in channel i can be expressed as

$$S(E_i) = \sum_m \tilde{R}_{im} \tilde{F}(\mathscr{E}_m), \tag{18}$$

where $\tilde{R}$ is the response function, a matrix whose m-th column is the spectrum corresponding to the discharge of the m-th level. Since the energy resolution is almost independent of the method of de-excitation of the level, the matrix $\tilde{R}$ can be expressed as a product of two matrices, one of which does not depend on the resolution if the distance between the levels is greater than the energy resolution or if columns of the matrix R differing little correspond to close-lying levels:

$$\tilde{R}_{im} = \sum_k R_{ik} \eta_{km},$$

where R is the response function in the limit of infinitely high resolution, and η is an operator that takes into

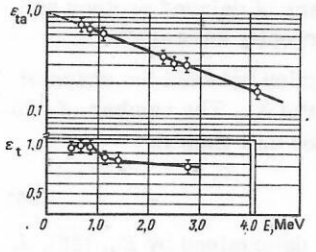

FIG. 16. Efficiency of total absorption ε_{ta} of the cascade of γ transitions and the efficiency of γ-ray detection for the total-absorption spectrometer.[41]

account the finite resolution of the instrument.

Equation (18) can then be rewritten in the form

$$S(E_i) = \sum_k R_{ik} F(F_k); \tag{19}$$

$$F(E_k) = \sum_m \eta_{mk} \tilde{F}(\mathscr{E}_m) \tag{20}$$

and solved in two stages. First, $F(E_k)$ is found from (19), i.e., the probability density for finite resolution, and then the distribution $\tilde{F}(\mathscr{E}_m)$ is obtained from (20).

To solve Eq. (19), it is necessary to know the matrix R_{ik}. This is a triangular matrix whose dimension is equal to the number of channels of the analyzer. It follows from the definition of the response function that

$$\sum_i \tilde{R}_{ik} = \sum_i R_{ik} = \varepsilon_T(E_k) \approx 1. \tag{21}$$

The diagonal elements are

$$R_{kk} = \varepsilon_{ta}(E_k) \tag{22}$$

and for a spectrometer with a pit they do not depend on the de-excitation scheme of the level. The nondiagonal matrix elements correspond to incomplete absorption of the cascade energy in the crystal and can depend on the decay scheme, so that in solving the system of equations (18) it is necessary to make assumptions about the method of de-excitation of the levels, though the conditions (21) and (22) mean that only the shape but not the area of the continuous distribution described by the nondiagonal elements of the matrix R can depend on the method of de-excitation. Therefore, if the nondiagonal matrix elements are incorrectly estimated, sections with negative area appear in the analyzed spectra. Since R is a triangular matrix, the contribution of the uncertaintly in the nondiagonal matrix elements to the error in the solution of Eq. (18) increases with decreasing energy of the levels. Therefore, if the conditions for ε_{ta} to be independent of the method of de-excitation are satisfied, the influence of the nondiagonal elements on the uncertainty in the level population probabilities will be greatest in the interval of energies from 0 to $E_{max}/2$, where E_{max} is the energy of the maximum in the level population probability density and, therefore, has little influence on S_β. In the analysis of the total-absorption spectra in Ref. 8, various methods of simulating the continuous distribution were compared, and the difference between the results was used to estimate the errors. For the main maximum and the high-energy levels the results of the analysis do not dependent on the method of de-excitation to more than 10%. Below the main maximum, the discrepancies may reach 100% for individual levels, but the total population of the low-energy levels also remains unchanged to within 10%, i.e., the total contribution of these levels to the strength function is hardly changed.

When the β^+-decay strength functions are used, it is very important to take into account detection of annihilation radiation. If a level with energy E_0 is populated by both electron capture and β^+ decay, then in the analyzed spectrum it corresponds to two peaks with energies E_0 and $E_0 + 2m_e c^2$, the ratio of their intensities being equal to the probability ratio ε/β^+. The introduction of cor-

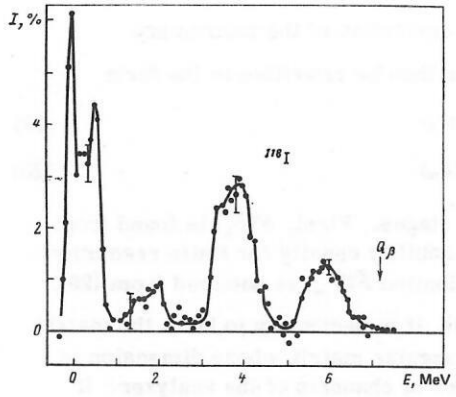

FIG. 17. Level population probabilities for decay of ^{118}I measured in Ref. 9 by the total-absorption method.

rections for the detection of annihilation radiation reduces to the solution of a system of linear equations with a two-diagonal matrix.[8] To raise the accuracy of its solution in the region $\varepsilon/\beta^+ \approx 1$, coincidences with positrons can be used.[10]

Additional distortions of the strength functions near Q are associated with the influence of the finite resolution of the spectrometer and the presence of random summation of pulses from different nuclei.[8]

Measurements of the level population probabilities in β^+ decay with a total-absorption spectrometer of large volume in 4π geometry[9] showed that the β^+-decay strength functions have a clear resonance nature. The probabilities for population of the ^{118}Xe levels following decay of ^{118}I obtained in Ref. 9 are given in Fig. 17. Comparison with Fig. 13 shows that the "sinuosity" of the strength function does indeed correspond to two isolated maxima—at 3.8 MeV ($\log ft = 5.3$) and 5.9 MeV ($\log ft = 4.4$) with width less than 1 MeV for instrumental resolution 10%.

In Refs. 8 and 10 the results are given of an investigation of the β^+-decay strength functions of deformed nuclei (Lu and Tm isotopes). The level population probabilities in percentages of the decays per channel and the β^+-decay strength function of ^{166}Lu are given in Fig. 18. The lower part of the figure gives the results of theoretical calculations in the Tamm-Dancoff approximation with a deformed Woods–Saxon potential. The spectrum contains numerous maxima with half-widths slightly exceeding the instrumental width. The calculations make it possible to interpret the structure of all the maxima in the strength function except for the peak at 3.5 MeV.[8] Figure 11 shows the β^+-decay strength function of ^{159}Tm. The lower part of the figure gives the theoretical strength function obtained in the random-phase approximation[10] "smeared" with a normal distribution with half-width 15%, which is close to the instrumental resolution. As can be seen from the figure, the ^{159}Tm strength function has the structure of a giant resonance—the main strength of the Gamow–Teller β^+ transitions is concentrated in an interval with a width of about 2 MeV, and more than 80% of the entire strength of the transitions is in the interval of energies

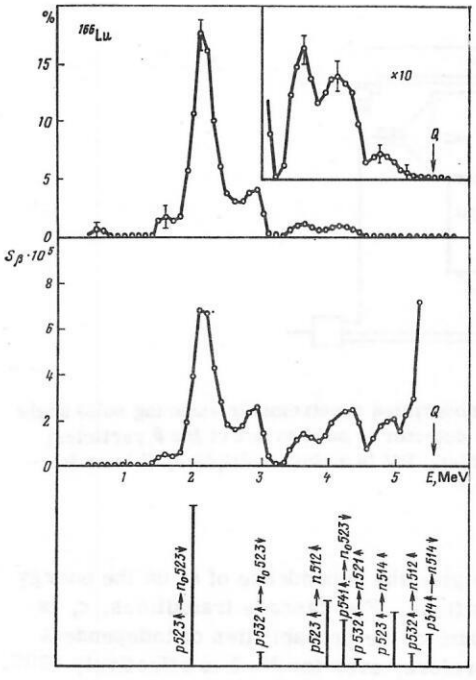

FIG. 18. Level population probabilities and S_{β^+} for decay of ^{166}Lu obtained by the total-absorption method in Ref. 8. The lower part of the figure gives the results of calculation of β-transition probabilities calculated in the Tamm–Dancoff approximation with Gamow–Teller residual interaction.

from 0 to Q, and, therefore, the ^{159}Tm strength function is the first example of direct observation of a giant Gamow–Teller resonance with $\mu_\tau = +1$ in the β decay of nuclei with $N > Z$.

4. INFLUENCE OF THE STRUCTURE OF THE BETA-DECAY STRENGTH FUNCTION ON THE SPECTRA OF DELAYED PROTONS AND ALPHA PARTICLES

If the energy E_i of a level populated by a β transition exceeds the proton or α-particle separation energy, this level may be de-excited by emitting protons or α particles. The energies of the delayed particles are determined by

$$E_i = B_x + E_f + \frac{A}{A - M_x} E_x;\ x \equiv \begin{cases} p; \\ \alpha; \end{cases} \qquad M_p = 1;\ M_\alpha = 4, \tag{23}$$

where B_x is the binding energy, E_x is the energy of the particle, E_i is the energy of the initial excited state, and E_f is the excitation energy after emission of the particle. More than 30 emitters of delayed protons and α particles with $T_z > 0$ are currently known.[5,42-44]

We shall consider the connection between the shape of the delayed-proton spectrum and S_β. The number of protons with energy E_p emitter per unit time is

$$I_p(E_p) = \sum_f I_\beta(E_i)\, \Gamma_p^{if}/\Gamma^i, \tag{24}$$

where the energy of level i is determined by Eq. (23), I_β is the probability of β transition to this level, Γ_p^{if}/Γ^i is the probability of proton emission (Γ_p is the proton width of the level, and $\Gamma^i = \Gamma_p^i + \Gamma_\gamma^i$ is the total width of

the level). The probability I_β is determined by the β-transition matrix element, i.e., by the strength function:

$$I_\beta(E_i) = C\eta(J_i) M_{GT}^2(E_i) f(Q - E_i). \quad (25)$$

where C is a normalization factor, η is a statistical factor (J_i is the spin of level i), M_{GT} is a reduced matrix element, and f is the Fermi function.

Equation (24) contains not only S_β but also the unknown Γ_p^i/Γ^i, and to extract information about S_β from the spectra of delayed protons the following assumptions are generally made:

1. The final state f in measurement of the shape of the proton spectra is not fixed, while in proton decay levels with energy up to 1 MeV are populated.[44] It is assumed that over an interval of about 1 MeV the variation in S_β can be ignored. This makes it possible to eliminate the summation over f in (27).

2. The ratio Γ_p/Γ is assumed to be uncorrelated to the probability of the β transition that populates this level. It is assumed that Γ and Γ_p depend only on the energy and on the level density and can be calculated in the statistical model.[43,44] In fact, it is assumed that the (β^+, p) process proceeds through compound states. Then (24) can be written in the form

$$I_p(E_p) \approx \text{const}\, S_\beta(E_i) f(Q - E_i) G(E_p), \quad (26)$$

where $G(E_p) = \langle \Gamma_p(E_p)/\Gamma(E_i) \rangle$ is the statistical mean of $\Gamma_p(E_p)/\Gamma(E_i)$. We note that assumption 1 is not confirmed experimentally, and assumption 2 appears very dubious.

The function f in (26) decreases as $(Q - E_p)^{-2}$ when $E_p \to Q$, the function G decreases exponentially as $E_i \to B_p$, and the spectrum of delayed protons has a characteristic bell shape with half-width that is usually 2–3 MeV. Therefore, the spectrum of delayed protons makes it possible to examine a fairly narrow interval of S_β.

The spectrum of delayed α particles has a similar form, but its maximum is shifted to lower energies $E_i + E_x + B_x$ because of the difference between the separation energies B_p and B_α.

From (24), we can estimate S_β:

$$S_\beta(E_i) = \text{const}\, \frac{I_x(E_x + B_x)}{f(Q - E_i) G(E_x)} = I_x(E_i)/R(E_x), \quad (27)$$

in which the value of the numerical constant depends on the probabilities of β decay to levels lying below B_x, and is generally not known. The function G depends very strongly on the parameters of the model (the level density, assumptions about the multipolarity of the γ transitions, the choice of the spin of the parent nucleus, the optical-potential parameters), but this expression can be used as a qualitative estimate of S_β; if the maximum in S_β is in the interval between B_x and Q, this must be reflected in the shape of the spectrum of delayed particles. Up to now, such an analysis has been made for 15 emitters in the region $A = 70$–180 (Table IV). In approximately half the cases, exceleent agreement with the statistical model $S_\beta = \text{const}$ is obtained, but in some cases, for example, ^{109}Te and ^{114}Cs, the discrepancy is very large. We now consider how the shape of the delayed-particle spectra is related to theoretical estimates of the positions of the peaks in S_β.[21]

TABLE IV. Emitters of delayed protons and α particles.

Nuclide	$T_{1/2}$, sec	b_p, %	B_p, MeV	Q, MeV	E_α, MeV	Shape of spectrum	Reference
^{73}Kr	25.9(6)	0.68(12)	2.0	6.9	6.1	Statistical	[45]
^{96m}Pd	14(1)	0.74(19)	—	8.5	5.5+E	—	[46]
^{109}Te	4.2(2)	—	1.5	8.6	5.9	Nonstatistical	[47]
^{111}Te	19.0(7)	—	2.3	7.4	6.1	—	[48]
^{113}Xe	2.8(2)	—	—	8.5	5.6	—	[49]
^{115}Xe	18(4)	0.34(6)	1.7	7.5	5.1	Nonstatistical	[50]
^{117}Xe	65(6)	0.29(6)	2.0	6.1	4.8	The same	[50]
^{114}Cs	0.57	7(2)	3.3	12.0	7.9	» »	[25]
^{116}Cs	3.5(2)	0.66	4.1	10.5	7.5		[42]
	0.65	0.28	—	—	—		
^{118}Cs	16.4(12)	$4.2\cdot10^{-2}$	4.9	9.6	7.1	Statistical	[51]
^{120}Cs	58.3(19)	$7\cdot10^{-6}$	5.6	8.9	6.6	The same	[44]
^{117}Ba	1.9(2)	—	—	8.9	5.0	Nonstatistical	[52]
^{119}Ba	5.4(3)	—	1.4	7.6	4.7	The same	[51]
^{121}Ba	29.7(15)	—	2.3	6.9	4.5	» »	[51]
^{129}Nd	6(3)	—	—	—	2.5	—	—
^{131}Nd	24(3)	—	—	—	2.5	—	—
^{133}Sm	3.2(4)	—	1.4	8.3	2.7	Statistical	[52]
^{135}Sm	10(2)	—	2.0	7.5	2.7	The same	—
^{179}Hg	1.09(4)	0.28	—	8.2	2.2	—	—
^{181}Hg	3.6(4)	$2\cdot10^{-2}$	1.31	—	3.3	Statistical	[45]
^{183}Hg	8.8(5)	$3\cdot10^{-4}$	1.85	—	3.3	The same	—
^{76}Rb	—	$4\cdot10^{-7}$	4.0	9.7	5.0	—	—
^{114}Cs	0.57	0.16	−2.8	12.0	7.9	Nonstatistical	—
^{116}Cs	3.5(2)	$3\cdot10^{-5}$	−2.0	10.5	7.5	The same	—
	0.65	$5\cdot10^{-4}$					
^{118}Cs	16.4(12)	$2.5\cdot10^{-3}$	−1.5	9.6	7.1	Statistical	—
^{120}Cs	58.3(19)	$2.0\cdot10^{-5}$	−1.0	8.3	6.6	The same	—
^{181}Hg	3.6(3)	$1.2\cdot10^{-5}$	−5.76	7.5	3.3	—	—

The β^+ Decay of Nuclides with $T_z = 1/2$. Nuclei with $T_z = 1/2$ are the lightest emitters of delayed protons with $T_z > 0$. So far, the proton spectra have been measured for the decay of ^{65}Ge, ^{69}Se, ^{73}Kr, and ^{77}Sr.[43] The shape of the ^{77}Sr spectrum is statistical. According to calculations, the energy of the maximum is 3 MeV, i.e., below B_p, and, therefore, the presence of the maximum does not influence the shape of the proton spectrum. The ^{73}Kr, ^{69}Se, and ^{65}Ge spectra have a nearly statistical shape, but they do contain narrow resonances with width around 0.2 MeV (Fig. 19). Calculations give for these nuclei a position of the main maximum at energy $Q = \pm 1$ MeV. Therefore, the main maximum is not populated by β^+ decay and does not influence the proton spectrum. Below Q, there are local maxima in S_β, and these are evidently manifested in the form of resonances in the proton spectrum.

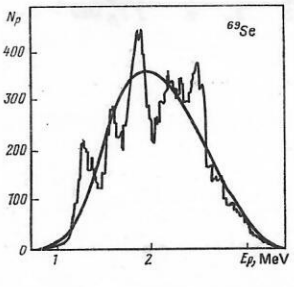

FIG. 19. Spectrum of delayed protons for the emitter ^{69}Se (histogram) compared with the predictions of the statistical model with $S_\beta = \text{const}$.

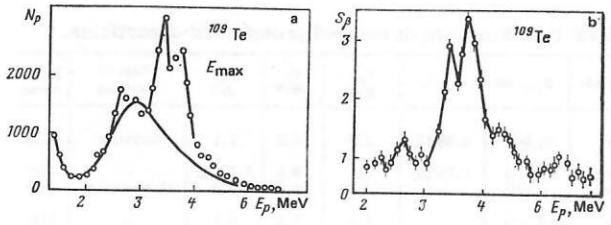

FIG. 20. Spectrum of delayed protons for decay of ^{109}Te (a) and the strength function S_β (b) obtained from it using Eq. (47).[47]

Nuclei of the $d_{5/2}$–$g_{7/2}$ Shell. The great majority of studies of emitters of delayed particles belong to this region. The conclusions drawn in the different studies are frequently contradictory with regard to the nature of the strength function even for the same emitter; many spectra have a clearly nonstatistical nature (^{109}T, ^{114}Cs, ^{116}Cs(α), ^{121}Ba; Figs. 20–22). However, ^{118}Cs has a statistical proton spectrum, and in ^{116}Cs the proton spectrum is statistical but the α-particle spectrum is nonstatistical. In the xenon nuclides ^{115}Xe and ^{117}Xe the population of the levels in the region of 6 MeV is appreciably less than in the region 4–5 MeV, but the shape of the spectrum is close to a statistical shape. As we noted above, the shape of a statistical spectrum depends very strongly on the parameters of the model (see Fig. 22), and it is customary to vary the parameters to achieve the best agreement with experiment; however, for ^{109}Te, ^{121}Ba, and ^{114}Cs no variation of the parameters can describe the experimental spectra under the assumption S_β = const of the statistical model.

We consider how the shape of the spectra is related to the position of the S_β maximum calculated in Ref. 21. In nuclei with $Z = 51$–64, the main maximum is associated with excitation of the states $(n_{g_{7/2}} - p^{-1}_{g_{9/2}})$ and $(n_{d_{3/2}} - p^{-1}_{d_{5/2}})$ and has excitation energy 4–8 MeV in the daughter nucleus. Table IV gives for all emitters the decay energies Q, the separation energies B_p and B_α, and the calculated position of the maximum E_{max}. The arrow in Figs. 19–22 indicates the energy E_{max} of the maximum. It follows from comparison of these experimental and calculated

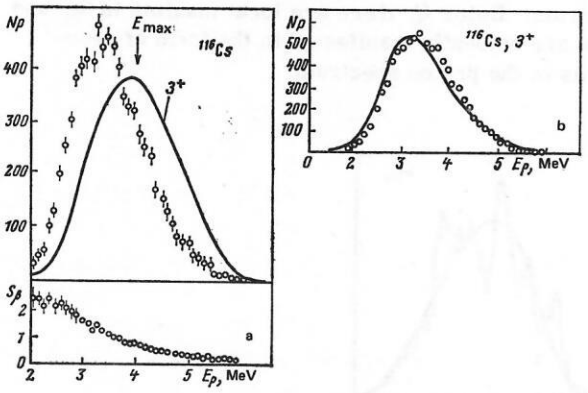

FIG. 21. Deviation of the shape of the delayed-proton spectrum from statistical shape: a) in accordance with the data of Ref. 42; b) in accordance with the data of Ref. 44.

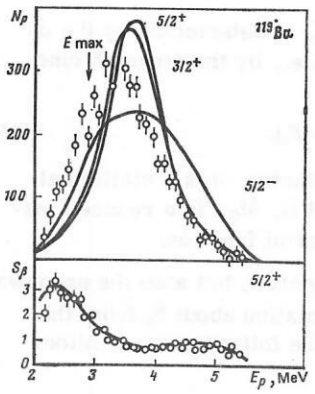

FIG. 22. Influence of assumptions about the quantum numbers of the ground state of the emitter ^{119}Ba on the shape of the function R.[51]

data that the shape of the spectrum is nonstatistical if the maximum in S_β coincides with the decreasing part of the function R. This is the case for ^{109}Te, ^{114}Cs, and ^{121}Ba. But if the maximum occurs in the "tail" of R, as, for example, in ^{118}Cs, then the shape of the spectrum is nearly statistical. The width of the function R is usually small, 1–2 MeV, i.e., comparable with the width of the maximum in S_β, and therefore if the position of the maximum in S coincides with the maximum in R, the shape of the spectrum is again nearly statistical, as in ^{118}Cs(α) and ^{120}Cs(α).

We consider the influence of the structure of S_β on the absolute probabilities of emission of delayed particles for the example of ^{114}Cs, which has decay energy 12 MeV. The spectra of the delayed particles are given in Fig. 9. The assumption S_β = const (broken curve) strongly contradicts the experimental data. It was assumed that S_β has the form of a constant + a Gaussian peak, and a least-squares determination of the parameters gave

$$S_\beta = 0.1 + 5\,(0.7\sqrt{2\pi})^{-1} \exp[-(E-8.15)^2/2\cdot 0.7^2]. \qquad (28)$$

This function is shown in Fig. 9c. For the absolute values of the probabilities of emission of delayed protons and α particles the values given in Table V were obtained.[25]

As can be seen from Table V and Fig. 9, for $S_\beta \neq$ const it is not possible to reproduce the experimental values of b_p and b_α, but one can correctly describe the shape of the spectra. For S_β = const, the probabilities can be correctly described, but the shapes of the spectra differ very strongly from what is observed. To find the origin of this discrepancy, we made calculations of the

TABLE V. Value of S_β for decay of ^{114}Cs.

I^π	S_β = const		$S_\beta \neq$ const*		Experiment	
	b_p	b_p/b_α	b_p	b_p/b_α	b_p	b_p/b_α
1^+	$4.1\cdot10^{-2}$	13	0.26	38	$7.2\cdot10^{-2}$	44 (20)
2^+	$4.2\cdot10^{-2}$	39	0.26	94	—	—
3^+	$3.9\cdot10^{-2}$	37	0.25	84	—	—

*Equation (28) without transitions to the ground state in β decay.

TABLE VI. Strength function for decay of ^{114}Cs.

E, MeV	B (GT)	lg ft	I, %	E, MeV	B (GT)	lg ft	I, %
2.8	0.05	5.4	3.8	8.6	1.0	4.1	0.53
5.0	0.20	4.8	4.1	9.3	0.2	4.8	0.05
6—7	0.20	4.8	1.8	10.0	0.5	4.4	—
7.9	2.2	3.7	2.7				

strength function of Gamow–Teller β transitions for the decay of ^{114}Cs using the deformed Woods–Saxon potential ($\beta_{20}=0.25$ and $\beta_{40}=-0.01$) in the random-phase approximation. The results are given in Table VI. Comparison of Figs. 9c and 9d shows that our calculations confirm the assumption made in Ref. 25 that S_β has a resonance nature. The estimates in Table V were made under the assumption that there are no β transitions to the ^{114}Xe ground state. According to our calculations the ^{114}Cs ground state has the configuration $(p_0[422]3/2-n_0[413]5/2)_{1^+}$, and therefore a strong transition to the ground state of the daughter nucleus is possible. The reduced transition probabilities between the ground states obtained in the calculations depend strongly on the choice of the model parameters, but if we use the experimental half-life of ^{114}Cs ($T_{1/2}=0.57$ sec according to Ref. 25) and the calculated values of the reduced probabilities for decay to the excited states, then for the transition to the ground state we obtain $I_{1^+\to 0^+}=85\%$ and $\log ft=5.0$, from which we find $b_\beta=0.04$, which agrees with the experiment.

Our analysis shows that calculations of the resonance structure of S_β make it possible to explain almost all the existing experimental data on the spectra of delayed particles. In some cases, measurement of the spectra of delayed protons and α particles makes it possible to obtain qualitative information about the shape of S_β. To obtain quantitative data, it is necessary to identify the proton decay channels leading to excitation of various levels of the nucleus $Z-2, N+1$, since otherwise the energy distortions may reach 1 MeV, i.e., may be comparable with the width of the delayed-particle spectrum. It would be of great interest to make a simultaneous measurement of the delayed-particle spectra and the total-absorption spectra.

5. ENERGY STRUCTURE OF THE β-DECAY STRENGTH FUNCTION OBTAINED FROM DELAYED-NEUTRON SPECTRA

The main maximum in the β^--decay strength function is situated a long way above the ground state of the parent nucleus and cannot be populated by β transitions—this is the main difference between delayed neutrons and delayed protons. However, for nuclei with sufficiently large neutron excess, back spin-flip states and core-polarization states may lie below the ground state of the decaying nucleus and, therefore, may be manifested in the delayed-neutron spectra. The reduced matrix elements for Gamow–Teller transitions to these states are usually large: $B_{1GT}\approx 1$.

Investigation of the spectra of delayed neutrons makes it possible to obtain a more detailed structure of S_β than

TABLE VII. Emitters of delayed neutrons.

Nuclide	$T_{1/2}$, sec	Q, MeV	B_n, MeV	b_n, %	Nuclide	$T_{1/2}$, sec	Q, MeV	B_n, MeV	b_n, %
^{84}As	5.60	9.99	9.06	0.061 (32)	^{92}Rb	4.50	7.80	7.35	0.125 (15)
^{85}As	2.03	9.05	4.10	60 (42)	^{93}Rb	5.86	6.62	5.14	1.164 (81)
^{86}As	0.90	11.35	6.22	7.1 (31)	^{94}Rb	2.71	9.45	7.71	9.6 (8)
^{87}Se	5.60	7.27	6.40	0.18 (4)	^{95}Rb	0.38	7.87	4.64	8.4 (5)
^{88}Se	1.52	6.33	4.85	0.57 (28)	^{96}Rb	0.20	10.76	6.62	13.0 (14)
^{89}Se	0.41	8.63	6.15	5.0 (15)	^{97}Rb	0.17	9.03	3.92	27.2 (30)
^{87}Br	55.7	6.68	5.46	2.55 (51)	^{99}Y	0.8	6.51	4.44	1.2 (8)
^{88}Br	15.9	8.98	7.15	5.5 (6)	^{134}Sb	11.0	8.70	7.35	0.11 (2)
^{89}Br	4.55	8.04	5.22	13.8 (34)	^{135}Sb	1.70	7.52	3.86	19 (3)
^{90}Br	1.63	10.33	6.21	22.6 (31)	^{136}Te	20.9	4.47	4.02	0.76 (1)
^{91}Br	0.65	9.18	4.57	9.9 (20)	^{137}Te	3.5	6.48	5.63	1.3 (8)
^{92}Br	0.25	12.01	6.21	16^{+16}_{-8}	^{137}I	24.6	5.79	4.45	6.1 (8)
^{93}Kr	1.29	8.15	6.30	1.92 (14)	^{138}I	6.55	7.80	5.80	2.58 (22)

is possible for delayed protons for the following reasons. Because there is no Coulomb barrier, the probabilities of emission of delayed neutrons when neutron-rich nuclei decay are appreciably higher than the probabilities of emission of delayed protons when neutron-deficient nuclei decay for the same values of E_i-B_x. In addition, the absence of the Coulomb barrier makes it possible to obtain S_β in the entire interval of energies from B to Q. Neutron-rich nuclides are usually obtained in fission reactions, which makes it possible to obtain emitters of delayed neutrons in quantities sufficient for the construction of the neutron decay schemes. The energy resolution in the measurement of neutron spectra is 12–40 keV.

So far, about 70 emitters of delayed neutrons have been identified.[42,53] The possibilities of neutron spectroscopy are revealed by Table VII. This shows that $\Delta=Q-B_n$, i.e., the energy interval that determines the maximal energy of the neutrons is a few mega-electron-volts for many emitters, and the total probabilities of neutron emission reach 20–60%, though the half-lives of such nuclides are fractions of a second, and the measurement of their spectra is a rather difficult problem. Up to now, probabilities for the population of levels by β decay have been obtained from measurement of the spectra of delayed neutrons and γ rays for ^{85}As, ^{87}Br, ^{135}Sb, ^{137}I, and $^{93-97}$Rb. A typical delayed-neutron spectrum (decay of ^{85}As) is shown in Fig. 23. Most of the intensity of the neutron transitions is in the form of clear peaks, which indicates the selective nature of β decay. For comparison, the same figure shows the shape of the neutron spectrum for $S_\beta=\text{const}$ and $S_\beta\sim\rho(E)$. The fairly high resolution makes it possible to construct the decay scheme of the excited states through the neutron channel.

If in the β decay of the emitter N, Z level i of the nucleus $N-1, Z+1$ is excited, and after neutron emission the levels f of the nucleus $N-2, Z+1$, then the probability of population of level i is

$$I_\beta^i=\sum_f \frac{\Gamma_n^i}{\Gamma^i} I_n(E_i-B_n-E_f), \tag{29}$$

where Γ_n is the neutron width of the level, $\Gamma=\Gamma_n+\Gamma_\gamma$ is the total width of the level, and $I_n(E)$ is the intensity of the line in the spectrum of delayed neutrons. The value of Γ_n/Γ is unknown, and it is therefore assumed that for all levels $\Gamma_n^i/\Gamma^i\sim\Gamma_n/\Gamma$. This mean value is estimated as follows. From the γ-ray spectrum, the in-

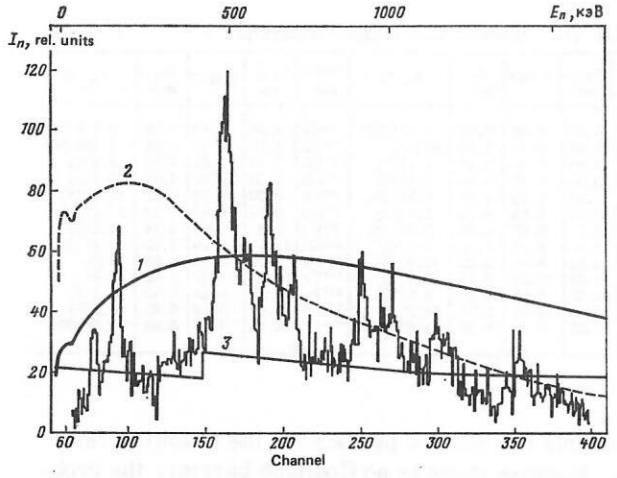

FIG. 23. Spectra of delayed neutrons (after correction for energy dependence of the detector efficiency) for the emitter ^{85}As. Curves 1, 2, and 3 give the shape of the spectrum in the statistical model with $S_\beta \sim \rho(E)$ for different parametrizations of the level density $\rho(E)$.[7]

tensities of transitions with energy $E_\gamma > B_n$ are estimated. Then

$$\left\langle \frac{\Gamma}{\Gamma_n} \right\rangle = \left\langle \frac{\Gamma_n + \Gamma_\gamma}{\Gamma_n} \right\rangle \approx 1 + \frac{\langle \Gamma_\gamma \rangle}{\langle \Gamma_n \rangle} \approx 1 + \frac{\sum_i I_\gamma}{\sum I_n}.$$

For the decay of As, for example, $\langle \Gamma_\gamma / \Gamma_n \rangle \geq 0.6$ was obtained[54] for levels with energy from B_n to $B_n + 1.5$ MeV; for ^{135}Sb, $\langle \Gamma_\gamma / \Gamma_n \rangle \geq 0.7$ was obtained in the interval from B_n to $B_n + 2.5$ MeV.

If $\Delta = Q - B$ is large, neutron decay may populate excited states of the nucleus $N-2, Z+1$, and in this case it is necessary to construct the neutron decay scheme. The levels of the nucleus $N-1, Z+1$ are introduced on the basis of the energies of the neutron transitions and the balance of the intensities of the neutron transitions that populate the level and the γ rays that de-excite it. Data on the neutron transitions for the decay of the excited states of ^{85}Se, the decay of ^{85}As, are given in Table VIII. It can be seen that the transition energies fit into the proposed decay scheme well. The final column gives the relative intensities of the neutron transitions obtained for the optical potential under the assumption that the nuclear matrix elements do not depend on the wave functions of the final states, i.e., there is complete mixing of the configurations, which is the basis of the statistical model of β decay. It can be seen from the table that transitions to the ground state are very strongly hindered, by more than 100 times, which contradicts the statistical model. This effect is explained in Ref. 22, in which, in the framework of the shell model with allowance for the residual Gamow–Teller interaction, calculations are made of the wave functions of the states of ^{85}Se, ^{87}Kr, and ^{135}Te populated by the β decay of the emitters ^{85}As, ^{87}Br, and ^{135}Sb, respectively. According to these calculations, the β^- decay of ^{87}Br can excite the single-particle neutron configurations $n_{p_{3/2}}$ and $n_{p_{1/2}}$, and, therefore, neutron decay to the ground state is allowed, which is confirmed by the experimental data[54]; almost the entire

TABLE VIII. Data on the decay of ^{85}As.[7]

E, MeV	$E-B$, keV	I_i	l_n	I_f	E_n (balance), keV	E_n, keV	I_n	
							experiment	optical potential
5.64	1518.6	5/2−	$p_{1/2}$	2_1^+	63	57 (1)	16	≡ 16
			$p_{5/2}$	0^+	1518	1524 (11)	20	73
6.51	2394 (3)	3/2−	$p_{1/2}$	2_2^+	272	274 (2)	15	24
			$p_{1/2}$	2_1^+	939	936 (4)	73	≡ 73
			$p_{3/2}$	0^+	2394	—	1	92
6.74	2623 (5)	1/2−	$p_{3/2}$	2_2^+	501	501 (3)	100	≡ 100
			$p_{3/2}$	2_1^+	1168	1168 (7)	36	120
			$p_{1/2}$	0^+	2623	—	1	108
6.77	2650 (4)	1/2−	$p_{3/2}$	2_2^+	528	522 (3)	87	≡ 87
			$p_{3/2}$	2_1^+	1195	1201 (8)	34	103
			$p_{1/2}$	0^+	2650	—	1	92
6.96	2840 (3)	5/2−	s	3^-	140	142 (3)	41	17
			$p_{1/2}$	2_2^+	718	716 (3)	51	≡ 51
			$p_{1/2}$	2	1385	—	5	71
			$f_{5/2}$	0^+	2840	—	1	16
7.67	3553 (7)	3/2−	s	2^-	254	248 (6)	5	10
			$d_{3/2}$	3^-	853	—	5	4
			$p_{1/2}$	2_2^+	1431	1437 (7)	40	≡ 40
			$p_{1/2}$	2_1^+	2038	—	1	42
			$p_{3/2}$	0^+	3553	—	0.1	40

neutron decay takes place to the ground state of ^{86}Kr. The decay of ^{135}Sb populates only three-particle configurations, mainly the state $\{p_{g_{7/2}}(n_{d_{3/2}}p_{d_{5/2}})_{1^+}\}_J$. Then if the ground state of the even–even ^{134}Te is taken to be the quasiparticle vacuum, the corresponding fractional-parentage coefficient $\langle \{p_{g_{7/2}}(n_{d_{3/2}}p_{d_{5/2}})_{1^+}\}_J \| a_n^+ \| 0 \rangle$ is equal to zero, whereas for transition to the 2^+ state

$$\langle \{p_{g_{7/2}}(n_{d_{3/2}}p_{d_{5/2}})_1+\}_J \| a_n^+ Q_2^+ \| 0 \rangle = c^2 u_{d_{5/2}}^2 \, 15 \begin{Bmatrix} 2 & 5/2 & 7/2 \\ 1 & J & 3/2 \end{Bmatrix},$$

where Q_2^+ is the operator of production of a quadrupole phonon, u is the coefficient of the Bogolyubov transformation, and C^2 is the weight of the configuration in the phonon wave function. The experimental data confirm this conclusion: For all levels populated in β decay, neutron decay to the ground state of ^{134}Te is hindered by at least 30–40 times.[54]

The β decay of ^{85}As can populate both single-particle neutron states and three-particle states.[22] The former can decay by neutron decay to the ground state,[74] but such decay is forbidden for the latter. As can be seen from Table VIII, it is only for the 5.64-MeV level in ^{75}Se that a strong neutron transition to the ground state was observed. Calculations predict that the energy of the single-particle neutron state $n_{p_{1/2}}$ is 5.5 MeV, and therefore it is preferable to ascribe the 5.64-MeV level the spin 1/2 and not 5/2. At high excitation energies there are three-particle configurations, for which decay to the ground state is forbidden. In the experimental spectrum, the hindrance reaches 4×10^2 (the 7.62-MeV level).

The above analysis permits a very important conclusion—the emission of delayed neutrons after β decay is a semidirect process and is very sensitive to the structure of the decaying states; therefore, there may be

strong correlation between the values of Γ_n, Γ_γ, and Γ_β, and the assumption that Γ^i/Γ^i_n is (29) can be replaced by some mean value contradicts the experimental data, and the data on the absolute probabilities of β transitions obtained from the spectra of delayed neutrons must be regarded as semiquantitative. However, the delayed-neutron spectra make it possible to study β decay to levels with energy up to 10 MeV, which hitherto has been inaccessible by other methods.

The β-decay strength functions of emitters of delayed neutrons obtained in Ref. 54 for ^{85}As, ^{87}Br, ^{135}Sb, and ^{137}I and in Ref. 55 for Rb isotopes are given in Fig. 5. The strength functions are plotted with a linear scale, which reflects the resonance structure better. The averaging interval is 0.5 MeV, i.e., of the order of the half-width of the resonances. The probabilities of β transitions are given in units of $B'_{GT} = 4\pi B_{GT}/G_A^2$ and are recalculated for the value $G_A = 0.56 g_A$,[56] where g_A is the coupling constant of the axial-vector interaction for the free nucleon. In the region below B_n, the strength functions were obtained from measurements of the γ-ray spectra. In the determination of the strength functions, the values of B_n and Q were calculated as mean values in accordance with various semiempirical formulas, which could strongly distort S_β in the region of high energies. The sharp rise in S_β for Sb near Q is evidently due to this uncertainty; for a change in $Q - B_n$ by 0.5 MeV leads to a change in S_β in the region of 6.5 MeV by 5–7 times.

These strength functions are distinguished by their resonance nature. In S_β for the rubidium isotopes there is a clear maximum with energy 3.5–4.5 MeV. When the decay energy is increased to 7 MeV, there appears a second maximum with energy 6 MeV, $B_{GT} = 1$–2. The origin of these resonances is explained in Ref. 22, which gives the results of calculations of the strength functions of Gamow–Teller transitions for the rubidium isotopes with $A = 89$–101. The maximum with energy 4 MeV is associated with back spin-flip transitions, and the maximum near Q with transitions to core-polarization states. The results of the calculations are compared with experimental data in Table IX. It can be seen from the table that the theory correctly describes the main features of the experimental strength functions. It is striking that the widths of the resonances are small, and the main contribution to the intensity of the maximum is made by a small number of levels.

In this paper, our approach to the analysis of the experimental data has been based on microscopic calculations. It should, however, be noted that in connection with the interpretation of data on delayed neutrons Hardy *et al.*[57,58] have attempted in a series of papers to show that the spectra of delayed neutrons satisfy merely statistical laws and that information about nuclear structure of nonstatistical nature cannot be extracted from them. Using the Monte Carlo method, they simulated the decay of a hypothetical nucleus—pandemonium—possessing only statistical properties. They showed that the retarded-neutron spectrum for the decay of pandemonium contains the same peaks as the spectra of the real nuclei. From this they deduced that

TABLE IX. Comparison of experimental and theoretical strength functions for the decay of various nuclides.[7,22]

Nuclide	Experiment			Calculation	
	E	$Q-E$	B_{GT}	$Q-E$	B_{GT}
^{89}Rb	3.6	1.0	0.27	1.5	0.32
^{91}Rb	4.1	1.6	0.68	2.3	0.56
^{93}Rb	4.1 6.0	3.4 1.5	0.24 1.90	3.5 —0.2 —2.0	0.61 0.76 0.60
^{95}Rb	4.1 5.75	4.6 1.9	0.46 1.10	4.2 —0.1	0.69 0.70
^{97}Rb	4.2 6.15	5.3 3.4	0.72 3.10	4.9 1.5	0.72 0.63
^{87}Br	5.3 6.7	1.5 0.1	0.36 0.20	2.0 —0.1 —0.2	0.05 (single-particle) 0.33 0.33
^{85}As	7.5	1.5	2.8	1.6 0.2 —0.5 —1.5	0.60 0.54 0.22 0.25
^{135}Sb	4.2 5.75 6.5	3.5 2.0 2.3	0.21 0.92 6.20	1.8 —0.9 —2.1	0.33 1.20 0.57
^{137}I	4.2 5.6	1.6 0.2	0.38 0.97	1.8 0.9 —2.1 —2.6 —3.6	0.33 1.2 0.57 0.24 0.24

the conclusion of a nonstatistical nature of the β decay cannot be drawn on the basis of the peaks in the retarded-neutron spectra. A detailed criticism of these papers is given in Ref. 7; here, we mention only one circumstance, which, in our view, is a decisive argument for the nonstatistical interpretation. It is true that the decay of the statistical nucleus may give rise to spectra with a structure very similar to the spectrum of a "nonstatistical" nucleus. There may be peaks and structures of the giant-resonance type. But the energy positions of these peaks and resonances for the "statistical" nucleus are random and are in no way correlated with the physical characteristics of nuclei. In the purely statistical model, it is also impossible for regularities to occur in the energy positions of the peaks on the transition from nucleus to nucleus. But the experimental data indicate such behavior in the energy positions of the maxima in S_β for both delayed neutrons[22] and other phenomena.[4] Thus, the maxima in S_β must be regarded as structures of giant-resonance type due to nuclear properties of nonstatistical nature.

6. INFLUENCE OF THE STRUCTURE OF THE β-DECAY STRENGTH FUNCTION ON THE PROBABILITY OF DELAYED FISSION

Delayed fission (fission after β decay[59]) has been intensively studied in recent years both in the Soviet Union and elsewhere. Study of delayed fission can yield information about the fission barriers of nuclei fairly far from the β-stability band, and for some nuclei this method of estimating the barriers is the only one currently available. Therefore, it is of interest to discuss

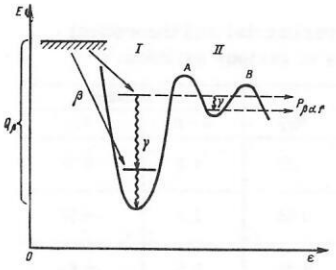

FIG. 24. Energy relationships for delayed fission.

the theoretical assumptions used to describe the process of delayed fission.

The probability of delayed fission is[60]

$$P_{\beta df} = \frac{\sum_i f(E_i) S_\beta(E_i) \Gamma_f(E_i)/\Gamma(E_i)}{\sum_j f(E_j) S_\beta(E_j)}, \quad (30)$$

where $f(E)S_\beta(E)$ is the probability of β decay to a level with excitation energy E, $f(E)$ is the Fermi function, $\Gamma_f(E)$ is the fission width of this level, and $\Gamma(E)$ is the total width of the level. The energy relationships are demonstrated in Fig. 24. It can be seen from the expression (30) that to predict the probabilities of delayed fission it is necessary to make certain assumptions about the shape of the β-decay strength function S_β. The β decay populates fairly simple configurations in the daughter nucleus, and in real nuclei these are fragmented over more complicated states. It is generally assumed that the fragmentation is fairly strong, which leads to strong mixing of the states and the disappearance of the structure in the β-decay strength function. In such an approach, one assumes $S_\beta = \text{const}$ or $S_\beta \sim \rho(E)$, where $\rho(E)$ is the level density of the daughter nucleus.[61] However, various experimental data discussed in the present paper indicate that the strength functions have indicate that the strength functions have an energy structure. As is shown in Refs. 33, 62, and 63, it is very important to take into account the structure of the β-decay strength function when analyzing delayed fission. To calculate S_β in Refs. 32, 62, and 63, a model first proposed in Ref. 27 and used in Ref. 14 to analyze the $M1$ γ decay of analog resonances was used.

Electron-Capture Strength Function and the Delayed Fission ^{232}Am $\rightarrow$ ^{232}Pu $\rightarrow f$. The nucleus ^{232}Am with half-life 44 sec decays into the nucleus ^{232}Pu, which fissions. The experimental probability[61] of the delayed fission is $P_{\beta df} = 1.3^{+4}_{-0.8} \times 10^{-2}$. The data on fission after ε capture of ^{232}Am were used in Ref. 61 to determine the inner fission barrier (A in Fig. 24) of the nucleus ^{232}Pu. The results of Ref. 61, which were obtained under the assumption $S_\beta = \text{const}$, were taken as proof of a large discrepancy between the height of the fission barrier extracted from delayed-fission data and calculated by Strutinskiĭ's method. However, the choice $S_\beta = \text{const}$ was not justified in Ref. 61, and it in no way reflects the specific nature of ε capture in the concrete case of the nucleus ^{232}Am. A calculation of the ε-capture strength function based on the assumption of charge-exchange excitations of Gamow–Teller type was made in Ref. 62. The single-particle states were chosen in accordance with the data of Ref. 64. The Hamiltonian of the system was expressed in the form

$$H = H_{sp} + H_{\text{int}}, \quad (31)$$

where H_{sp} is the Hamiltonian of the model of independent quasiparticles, and H_{int} is the residual interaction:

$$\left.\begin{aligned} H_{\text{int}} &= G_{\tau\sigma}(\sigma\sigma)(\tau\tau); \\ G_{\tau\sigma} &= 50/A; \end{aligned}\right\} \quad (32)$$

$G_{\tau\sigma}$ is measured in mega-electron-volts, and A is the number of nucleons in the nucleus. In the Tamm–Dancoff approximation, the secular equation corresponding to diagonalization of (31) is

$$\sum_i \frac{A_i^2}{E - E_i} = \frac{1}{G_{\tau\sigma}}, \quad (33)$$

where A_i are the excitation amplitudes, and E_i is the energy of the np excitation, the spin of the parent nucleus being assumed to be 1^+. Solving this equation, we find the energy E. Then for the strength function we have

$$S_\beta(E_j) = \frac{2J_j+1}{2J_i+1}\left(G_{\tau\sigma}\sum_i \frac{A_i^2}{(E_j - E_i)^2}\right)^{-1}. \quad (34)$$

The results of the calculation are given in Table X.

The energies in this table are calculated from the ground state of the daughter nucleus. For the calculation of $P_{\beta\,df}$, it is sufficient to know the strength function S_β up to a constant factor, since it cancels, and therefore $S_\beta = \text{const}\, B$.

Estimates of the Fission Barriers of the Nuclei ^{232}Pu, ^{244}Cf, ^{248}Fm, ^{248}Cf, and ^{240}Cm. The barrier for ^{232}Pu was determined under the assumption $S_\beta = \text{const}$ in Ref. 61, which found a significant discrepancy between the barriers—the theoretical barrier calculated by Strutinskiĭ's method and the barrier deduced from the data on the delayed fission of ^{232}Pu. In Refs. 62 and 63, the probabilities of delayed fission of ^{232}Pu, ^{244,248}Cf, ^{248}Fm, and ^{240}Cm were estimated with an ε-capture strength function that takes into account the structure of the nucleus and consists of Gaussian peaks centered on the levels 0^+ and 2^+ (see Table X) with half-width 1 MeV. The peak-to-background ratio was taken to be 100. This half-width and background correspond to the experiments on delayed neutrons. For the fission barriers, we take the theoretical values of Ref. 65. The delayed-fission probabilities were calculated by a program similar to the one used in Ref. 61. The process of fission through a double-hump barrier was calculated in accordance with a model that takes into account partial

TABLE X. Strength function of ε capture for ^{232}Am.[62]

J^π	E, MeV	B_{GT}
0^+	0	0.14
0^+	2.47	1.75
2^+	0.64	0.06
2^+	2.40	7.79

TABLE XI. Results of calculations of $P_{\beta df}$.[33]

Nuclides	$P_{\beta df}$	
	Experiment (Refs. in square brackets)	Theory
^{232}Pu	$1.3^{+4}_{-0.8}\cdot10^{-2}$ [61]	$5\cdot10^{-3}$
^{244}Cm	$5\cdot10^{-4}$ [70]	$4\cdot10^{-4}$
^{248}Fm	$3\cdot10^{-3}$ [70]	$2\cdot10^{-3}$
^{240}Cm	10^{-5} [70]	$9\cdot10^{-7}$
^{248}Cf	10^{-7} [70]	$2\cdot10^{-7}$

mixing of the states in the first and second wells.[66] As a result, the probability of delayed fission for ^{232}Pu was found to be $P_\beta = 5\times10^{-3}$. The experimental value is $P_{\beta df} = 1.3^{+4}_{-0.8}\times10^{-2}$.[61] Since the experimental and theoretical values agree, it follows that there are no grounds for asserting that the fission barriers calculated by Strutinskiĭ's method do not correspond to the delayed-fission data for ^{232}Pu. In Refs. 62 and 63, estimates were also made of the delayed-fission probabilities for the nuclides ^{244}Cf, ^{248}Cf, ^{240}Cm, and ^{248}Fm, allowance being made for the structure of the nuclei in the strength functions. The fission barriers were taken from Ref. 65. The results of the calculations[7] are given in Table XI and in Fig. 25.

The results of the calculations[63] given in Table XI agree well with the experiment, but it should be noted that in the calculation in Ref. 63 the nuclei were assumed to be spherical, and it would therefore be of great interest to calculate S_β with allowance for deformation.

Comparison of Different Models for Calculating $P_{\beta df}$. In Ref. 63, the delayed-fission probabilities were estimated by means of a model of fission through a double-hump barrier that presupposes partial mixing of the states in the first and second wells.[66] We now consider the process of delayed fission through a double-hump barrier and compare the $P_{\beta df}$ values obtained in different models. Such a comparison was made in Ref. 67.

The method of calculating fission through a double-hump barrier depends on the relationships between D_I, D_{II}, and W,[68] where D_I is the distance between the levels that correspond to internal nonfission degrees of freedom, D_{II} is the distance between the levels of the fission mode, and W is the width of levels of class II, determined by the width of decay through the inner barrier A and the outer barrier B.

The process of delayed fission can be represented schematically as follows. After β decay, the nucleus is in an excited state. Because of the mixing of the fission mode with the inner modes (mixing of the states of the classes I and II), the nucleus fissions. The fission mode may be mixed with the internal modes in both the potential wells, I and II. Decay of the fission mode to the internal degrees of freedom in the second well, damping, is ensured by a corresponding imaginary correction to the fission potential. When the fission mode decays to the internal modes, rotational states can be excited with different values of K, which is the projection of the total angular momentum of the axisymmetric nucleus onto the symmetry axis. Allowance for this K mixing is important in the analysis of the angular distribution of the fission fragments, but is not so important in the calculation of the total fission probability.[68] The following circumstance[69] should be noted. In the calculation of fission through a barrier, it is necessary to calculate the ratios of the widths of various processes, for example, $\Gamma_f(E)/\{\Gamma_f(E)+\Gamma_\gamma(E)\}$, where $\Gamma_f(E)$ is the fission width at energy E, and Γ_γ is the γ-decay width. Introducing the averaging factor F,[69] we can write

$$\left\langle \frac{\Gamma_f(E)}{\Gamma_f(E)+\Gamma_\gamma(E)} \right\rangle = F\frac{\langle\Gamma_f(E)\rangle}{\langle\Gamma_f(E)\rangle+\langle\Gamma_\gamma(E)\rangle},$$

where $\langle\ \rangle$ denotes averaging over the energy interval D_{II}. In calculations with $S_\beta = \text{const}$, one frequently takes $F = 1$.[68] Estimates of F are given in Ref. 69, and it is found that by assuming $F = 1$ one can obtain an incorrect result for the fission barrier. Taking the experimental probability of delayed fission for ^{232}Pu equal to $P_{\beta df} = 5\times10^{-3}$, Izosimov and Naumov[67] found the fission barriers of ^{232}Pu for different models of fission through a double-hump barrier and different assumptions about the nature of the β-decay strength function.

The results are given in Table XII. Comparing the data in Table XII, we can conclude that for the calculation of the probability of delayed fission of ^{232}Pu the shape of the strength function influences the result more

TABLE XII. Fission barrier of ^{232}Pu from the data of delayed fission.[33]

Barrier height	$S_\beta = \text{const}$			$S_\beta \neq \text{const}$ [62]		
	a (Ref. 61)	b	c	d (Ref. 62)	e	f
E_A, MeV	5,6	5.8	5.8	—	4.4	4.4
E'_A, MeV	5.5	5.8	5.6	$E_A = 3.5$ MeV, $E_B = 4.2$ MeV	$\leqslant 3.8$	$\leqslant 3.8$

Note. E_A for the outer barrier, $E_B = 4.0$ MeV; E'_A for the outer barrier, $E_B = 4.5$ MeV; a) $S_\beta = \text{const}$, partial summation of the fission mode and internal mode in the first and second well; b) $S_\beta = \text{const}$, no damping of the fission mode in the second potential well, WKB approximation for the barrier penetrability, and averaging factor $F = 1$; c) $S_\beta = \text{const}$, so damping of the fission mode in the second potential well, WKB approximation, the factor F calculated; d) S_β found from model with Gamow–Teller residual interaction, partial mixing of the fission mode and the internal mode in the first and second potential wells; e) S_β from Ref. 62, complete damping of the fission mode in the second potential well; f) S_β from Ref. 62, no damping of the fission mode in the second potential well, penetrability in WKB approximation.

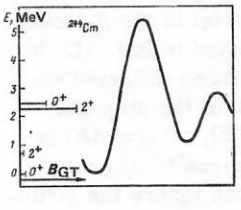

FIG. 25. Fission barrier and S_β for ^{244}Cm.[63,65]

TABLE XIII. Results of calculation of $P_{\beta df}$ for ^{236,238}Pa.

Nucleus	$S_\beta = \text{const}$	$S_\beta \sim \rho(E)$	Model[14]	Experiment
^{236}U	$6\cdot10^{-7}$	$6\cdot10^{-4}$	10^{-12}	10^{-9}
^{238}U	$2\cdot10^{-5}$	10^{-2}	10^{-8}	10^{-8}

strongly than the model used to calculate the process of fission through the barrier.

The β^--Decay Strength Function and the Delayed Fission ^{236,238}Pa $\rightarrow$ ^{236,238}U $-f$. For β^+ decay, or ε capture, the Hamiltonian (31) is diagonalized in a basis of neutron–particle–proton-hole excitations coupled to angular momentum 1^+. In the case of β^- decay, the basis is composed of proton–particle–neutron-hole excitations coupled to 1^+.

The probability of delayed fission of the nuclei ^{236,238}Pa was measured in Refs. 60, 70, and 71. To calculate $P_{\beta df}$, the β^--decay strength function for the decay of ^{236,238}Pa was calculated in Ref. 33. The basis configurations included two-particle configurations, core-polarization states, and spin-flip and back spin-flip states. Calculations were made under the assumption that the nuclei have spherical shape. Further, the probability of delayed fission was calculated in Ref. 33 under different assumptions about the shape of the β-decay strength function, and the results of the calculations were compared with the experimental values of $P_{\beta df}$. The results are given in Table XIII.

It can be seen that if the assumptions $S_\beta = \text{const}$ or $S_\beta \sim \rho(E)$ are made, then $P_{\beta df}$ values greatly exceeding the experimental ones are obtained. If S_β calculated in accordance with the model in Ref. 14 is used, the $P_{\beta df}$ values agree better with the experiment. The qualitative nature of S_β is not changed by variation of the parameters of the theory over small ranges. The structure of S_β has the following features (Fig. 26). Below the ground states of ^{236}Pa and ^{238}Pa there is a small fraction of the total strength of the β^- transitions. The main contribution to the delayed-fission probability is made by states whose energies lie in the interval from the ground state of the parent nucleus to the bottom of the second potential well of the fission barrier. This interval is 0.6 MeV for ^{236}P and 1.4 MeV for ^{238}Pa. It should be noted that without any fitting of the parameters of the model the states making an appreciable contribution to the delayed-fission probability occur in this interval. The β^--decay strength function of the ^{238}Pa nucleus[33] is shown in Fig. 26, and the fission barriers used in the calculations are also shown. It should be noted that for ^{236}Pa and ^{238}Pa both barriers A and B have an important influence on the delayed-fission probability, in contrast to ^{232}Pu, and therefore the calculation of $P_{\beta df}$ is more sensitive to the choice of the model used to calculate the fission through the double-hump barrier. In Ref. 33, the simplest model of fission through a double-hump barrier was proposed. In the calculation of $P_{\beta df}$, it is necessary to calculate the ratio $\Gamma_f(E)/\Gamma(E)$, where Γ_f is the fission width of the level, and $\Gamma(E)$ is its total width.

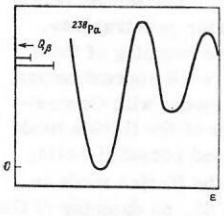

FIG. 26. Fission barrier and S_β for ^{238}Pa.[33]

7. INFLUENCE OF THE STRUCTURE OF THE β-DECAY STRENGTH FUNCTION ON THE FORMATION OF HEAVY AND SUPERHEAVY NUCLEI IN ASTROPHYSICAL PROCESSES

The relative abundances of the nuclei of the various isotopes found in our region of the Universe exhibit a number of regularities that can be attributed to the properties of the astrophysical processes in which these elements were synthesized. Heavy nuclei, i.e., nuclei heavier than iron, were evidently formed by the capture of neutrons and subsequent β^- decay.[11] If the capture of neutrons takes place more rapidly than the β decay, then neutron-rich nuclei are formed, and their appreciable abundances in the solar system indicate that an important part is played by the process of rapid capture of neutrons (the r process) in the evolution of matter in the Universe.[11] After the r process, which may occur, for example, during a supernova explosion,[75] the synthesized neutron-rich nuclei decay to the β-stability band, the numbers of nuclei of the various isotopes near it depending on the competition between the following processes: β^- decay, the emission of delayed neutrons, delayed fission, γ decay, etc.[76] As a result of the stellar r process, one cannot rule out the formation of superheavy nuclei,[77] whose numbers will depend on the probabilities of the delayed processes.[78] Delayed fission may contribute to the energy balance in the evolution of supernovae.[79]

For the verification of cosmological models, it is important to estimate the time scales of the evolution of the Universe. In estimates of times of this type, one uses the ratios of the abundances of definite isotopes; such chronometric pairs[80] are ^{238}U/Th, ^{235}U/^{238}U, and ^{244}Pu/^{232}Th. Delayed fission is rather important in the formation of chronometric pairs and is estimated in Ref. 76. However, none of the papers quoted above took into account the structure of the β-decay strength function. In Refs. 22, 33, and 62 it was shown how important it is to know this structure when determining the probabilities of delayed fission and the emission of delayed neutrons. The importance of taking into account the structure of the strength function $S_\beta(E)$ in calculations of the rates of formation of nuclei in the β-decay chain after capture of neutrons is noted in Ref. 81. In calculations of delayed processes, three different assumptions are made about the shape of the strength function: 1) $S_\beta = \text{const}$[82-84]; 2) $S_\beta \sim \rho(E)$, where $\rho(E)$ is the level density in the daughter nucleus[78]: 3) gross theory.[85] All these three assumptions ignore the structure of the strength function, which has a strong influ-

ence in the calculation of the probabilities of delayed fission and the emission of delayed neutrons.

Structure of the β^--Decay Strength Function of Heavy Neutron-Rich Nuclei. In connection with what we have said above, it is of interest to calculate S_β with allowance for the structure of the nucleus using the model proposed in Ref. 14, and to estimate the rates of formation of the nuclei in the β-decay chain after the r process. It should be noted that in the calculation of the probabilities of delayed processes for nuclei formed as a result of the r process it is necessary to make rather far extrapolations to nuclei at considerable distances from the stability band. Although the results of such estimates are very sensitive to the choice of the extrapolation (this applies particularly to the fission barriers), such a calculation nevertheless shows the necessity of taking into account the structure of S_β. In Refs. 34 and 86, S_β was calculated in accordance with the model proposed in Ref. 14 and used earlier to calculate delayed processes. The deformation of the nuclei was assumed to be zero. It was found that for nuclei with $A = 250-266$ and $N = 165-175$ (parent nucleus) S_β can be represented in the form

$$S_\beta(E) = \text{const}\ \delta(E - E_i).$$

The dependence of E_i (MeV) on N and Z is well described by the expression

$$E_i = -0.15(N - 160) + 0.46(Z - 88) - 0.31 \quad (35)$$

or

$$E_i = -0.15(N - 160) + 0,46(Z - 88) - 2.9, \quad (36)$$

where Z is the number of protons in the parent nucleus.

For (35) and (36), different energies of the spin–orbit splitting were taken. In these expressions, the energy is measured from the ground state of the parent nucleus. These dependences can be extrapolated as far as $N = 200$.

Formation of Chronometric Pairs and the Structure of $S_\beta(E)$. We shall discuss the influence of the structure of $S_\beta(E)$ on the probabilities of formation of the chronometric pairs $^{238}U/^{232}Th$, $^{235}U/^{238}U$, and $^{244}Pu/^{232}Th$. All the information about the age of the chronometric pairs is contained in the parameter $R(i,j) = (P_i/P_j)(N_i/N_j)$ and the half-lives of the nuclei forming the pair. Here, P_i/P_j is the ratio of the numbers of nuclei after the series of β decays that follow the r process; N_i/N_j is the ratio of their numbers at the present time. Strictly speaking, the parameter R is not model-independent, since the ratio P_i/P_j depends on the dynamics of the r process and also on the subsequent irradiation by neutrons.[76]

In Ref. 87, in which it was assumed that nuclei with $A = 232-256$ are formed in the r process in equal numbers, Schramm obtained the ratios P_i/P_j, which are regarded as standard, and gave possible errors for P_i/P_j. However, he did not take into account delayed fission. Estimates of P_i/P_j with allowance for delayed fission were made in Ref. 76. It was found that in the region of $A \approx 244$ the probability of delayed fission is appreciable, $P_{\beta df} = 0.46$, which entails a decrease in the formation of ^{235}U and ^{244}Pu, and therefore P_i/P_j for $^{244}Pu/^{232}Th$ and $^{235}U/^{238}U$ is significantly reduced (by 30–40%), whereas P_i/P_j for $^{232}Th/^{238}U$ is reduced much less. However, the calculations of the delayed-fission probabilities in Ref. 76 were made under the assumption $S_\beta \sim \rho(E)$. For this strength function, the fraction of delayed fission in the region of $A \approx 244$ is determined by the fractions of the β transitions to the energy interval about 1 MeV below the ground state of the parent nucleus. If S_β is taken from Ref. 86, then almost 100% of the strength of the Gamow–Teller decays is in this interval, and further advance along the chain is possible only by virtue of the "tails" of the strength function of the Gamow–Teller transitions or first-forbidden transitions or the emission of delayed neutrons. Thus, the ratio P_i/P_j for $^{244}Pu/^{232}Th$ and $^{235}U/^{238}U$ may be significantly reduced. Detailed calculation of delayed fission is made difficult by the fact that the properties of many nuclei far from the stability band are not known.

Delayed Fission and the Formation of Superheavy Nuclei. It is possible that as a result of a series of β decays following the r process nuclei with $A \approx 300$ and long half-lives, i.e., superheavy nuclei,[77] could be formed. A model taking into account the influence of delayed fission on the formation of such nuclei was proposed in Ref. 78. The chain of β decays of the nuclei formed in the r process can be divided into four parts[78]: 1) in the immediate proximity of the path of the r process, the emission of delayed neutrons is dominant; 2) the emission of delayed neutrons and delayed fission have comparable probabilities; 3) delayed fission and β decay have comparable probabilities; 4) β decay is dominant.

At the beginning of the chain of β decays, Q_β is very large, almost all daughter nuclei are formed in highly excited states, the neutron separation energy is low, and the emission of delayed neutrons is dominant. Subsequently, Q_β decreases, B_n increases, and the probability of delayed fission increases. In the region $A \approx 294$, delayed fission is about 99%, and it can reduce the numbers of superheavy elements by 3–200 times.[78] In the calculation of the probabilities of delayed fission in Ref. 78 it was assumed that $S_\beta \sim \rho(E)$, but if allowance is made for the structure of the strength function the conclusions drawn in Ref. 78 may be changed. The strength function S_β calculated in Ref. 86 has one maximum, whose centroid moves away from the ground state of the parent nucleus with increasing distance from the β-stability region. It may well be that for $A \approx 294$ delayed fission is less than for $S_\beta \sim \rho(E)$, and the influence of it on the probabilities of formation of superheavy elements is less. It is also necessary to investigate the competition between the α and β decay processes.

8. GAMOW–TELLER RESONANCE FROM THE (p,n) REACTION

It is easy to show that a direct single-step reaction must lead to population in the final nucleus of charge-exchange nuclear excitations. By means of such reac-

tions, analog states were discovered and the isotopic dependence of the optical potential was studied in the middle of the sixties. However, the transition to the Gamow–Teller resonance occupied more than 10 years, and it was only in 1980–1981 that systematic data on the Gamow–Teller resonance in the (p,n) reaction appeared. The reasons for this are to be sought in the higher requirements on the experimental techniques needed to investigate the Gamow–Teller resonance as compared with those used to investigate analog resonances. Analog resonances appear as dominant peaks in the spectra of neutrons from the (p,n) reaction at proton energies 30–50 MeV in a fairly wide range of angles. At such energies, the Gamow–Teller resonance is manifested weakly. With increasing proton energy, the ratio of the population intensities changes in favor of the Gamow–Teller resonance. At proton energies 100–200 MeV and especially at angle $0°(L=0)$ the dominant peak in the spectrum is the Gamow–Teller resonance.

Systematic experimental investigations of the Gamow–Teller resonance ($\mu_\tau = 1$) were made using the monochromatic cyclotron of the State of Indiana at proton energies 100–200 MeV. The neutron spectrum was measured by the time of flight (base length 60–70 m). The energy resolution was 140 keV. Details of the experimental technique can be found in Refs. 88–91.

At the beginning of 1981, data of various kinds were published on measurements of the neutron spectrum at angle 0° in the (p,n) reaction in the region of the Gamow–Teller resonance for targets from Li to Pb.[23] However, a quantitative analysis was not made for all the data. In many cases, only the energies of the peaks observed in the neutron spectra are known. For some cases, the nuclear matrix elements $\langle GT \rangle$ were obtained. Reference 99 gives the energies of the maxima in the neutron spectrum for the reaction $^{48}Ca(p,n)^{48}Sc$ ($E_p = 160$ MeV), and in Ref. 100 they are given for the reaction $^{90}Zu(p,n)^{90}Nb$($E_p = 120$ MeV). In Ref. 101, there is a discussion of the energy systematics of the Gamow–Teller resonances for the targets $^{90-92,94,96}Zr$, ^{93}Nb, $^{94,96-98,100}Mo$, $^{112,116,120,122,124}Sn$, and ^{208}Pb($E_p = 45$ MeV). Reference 102 gives the energy systematics of the Gamow–Teller resonance for the targets $^{90,92,94}Zr$, $^{112,116,124}Sn$, ^{169}Tu, and ^{208}Pb($E_{p_{208}} = 120, 160, 200$ MeV). In Ref. 24, data are given for the reaction $^{208}Pb(p,n)$-^{208}Bi($E_p = 120$ MeV). Widths of the Gamow–Teller resonance are given in Refs. 24 and 99–101. Matrix elements for ^{90}Zr and ^{208}Pb are given in Refs. 100 and 24, respectively. Typical neutron spectra are shown in Figs. 6, 7, and 27. The characteristic features of the experimental data are the following:

1. The neutron spectra of the (p,n) reaction at 0° contain not only the analog resonance but also other resonances whose cross sections are comparable with or greater than the IAR cross sections. When the proton energy is increased from 100 to 200 MeV, the relative IAR population cross section decreases.

2. At excitation energies below the analog resonance, a strong 1^+ peak is observed for targets with $A < 90$. This peak can be interpreted as a core-polarization state.

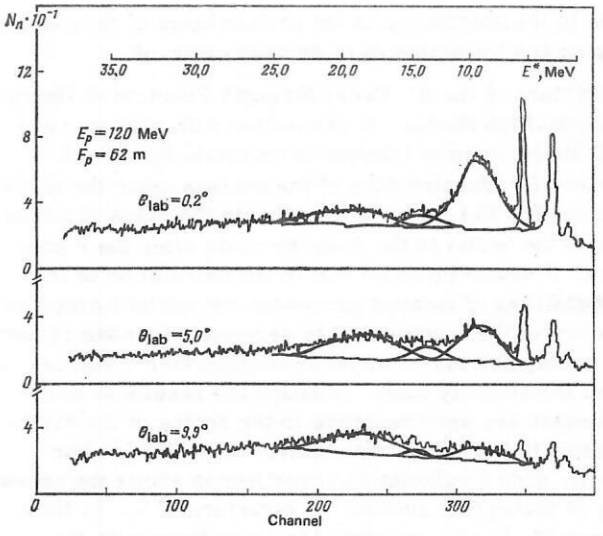

FIG. 27. Spectrum of neutrons from the $^{90}Zr(p,n)$ reaction.[100]

3. At excitation energies above the IAR, a 1^+ giant Gamow–Teller resonance is observed.

4. At even higher excitation energies, one can identify a $T_>$ part of the Gamow–Teller resonance.

5. In the neutron spectra at around 4.3° a 1^- charge-exchange resonance can be identified.

6. In accordance with Ref. 102, the excitation energy of the Gamow–Teller resonance is well described by

$$E_{GT} - E_{IAR} = (6.7-30.0\,(N-Z)/A)\ \text{MeV}.$$

7. The width of the Gamow–Teller resonance (FWHM) is between 2 and 4 MeV.

8. The value of $\langle GT \rangle^2$ for the Gamow–Teller resonance is 8.3 for the ^{90}Nb nucleus[100] and 48 for ^{208}Bi.[24]

The position of the Gamow–Teller resonance was calculated in a model with residual interaction in Ref. 103. The model[14,22] used to calculate the position and population intensity of the Gamow–Teller resonance is a schematic model that takes into account the isospin–isospin and spin–isospin residual interaction:

$$H_{int} = G_\tau(\tau_1\tau_2) + G_{\tau\sigma}(\tau_1\tau_2)(\sigma_1\sigma_2).$$

This model was originally used to analyze $M1$ γ decay of analog resonances.[4,14,32] the β-decay strength functions from the spectra of delayed neutrons,[22] and the intensities of delayed fission.[33] In all cases, the positions and population intensities of the Gamow–Teller resonance were calculated: for As isotopes in Ref. 32, for Rb in Ref. 22, and for Pa isotopes in Ref. 33. In Ref. 34, the position and population intensity of the Gamow–Teller resonance were calculated for a large number of nuclei with $A = 250-266$, $N = 165-175$. In Refs. 8 and 21, the model was used to calculate the position of the Gamow–Teller resonance ($\mu_\tau = +1$) in connection with experimental data on the β^+-decay strength functions of neutron-deficient nuclei, and in Ref. 62 in connection with analysis of data on delayed fission.

For the present paper, we have calculated the position of the Gamow–Teller resonance for a number of even–even parent nuclei used as targets for the (p, n) reaction. The Gamow–Teller resonance is in a neighboring odd–odd nucleus. In the simple model we have employed, it is necessary to specify the constants of the charge-exchange interactions G_τ and $G_{\tau\sigma}$ and the spin–orbit splitting of the single-particle states. The calculation was made for $G_\tau = 50/A$ MeV and $G_{\tau\sigma} = G_\tau$ and $G_{\tau\sigma} = (2/3)G_\tau$. For the spin–orbit splitting, we used the expression

$$\Delta E_{ls} = \frac{10}{A^{2/3}}(2l+1)$$

(ΔE_{ls} is measured in MeV).

For each nucleus, we calculate the β^--decay strength function, which has a well-defined peak (Gamow–Teller resonance with $\mu_\tau = -1$). The energy is measured from the analog resonance. The results of the calculations are given in Table XIV and in Fig. 28, which gives the energies of the Gamow–Teller resonance and the core-polarization states. We note some general features obtained in the calculations:

1. In all the nuclei, the Gamow–Teller resonance is situated above the analog of the ground state of the parent nucleus. The distance from the analog to the Gamow–Teller resonance varies smoothly with the atomic number of the target nucleus from 4–5 MeV for light nuclei to about 1 MeV for heavy nuclei (see Fig. 28).

TABLE XIV. Postion of Gamow–Teller resonance calculated in a model with spin–isospin residual interaction.[103]

Target nucleus	E (GT), MeV	Target nucleus	E (GT), MeV	Target nucleus	E (GT), MeV	Target nucleus	E (GT), MeV
^{22}Ne	9.3 −3.0	^{58}Ni	8.6 −1.4	^{90}Zr	3.4 −4.4	^{141}Nd	1.8 −7.3
^{24}Mg	8.2 −3.4	^{60}Ni	6.9 −2.7	^{92}Zr	3.0 −5.4	^{152}Sm	1.8 −7.7
^{26}Mg	10.2 −3.0	^{62}Ni	5.5 −4.2	^{94}Zr	2.7 −6.3	^{190}Os	1.0 −8.9
^{30}Si	1.2 −1.7	^{64}Ni	4.0 −5.5	^{98}Mo	3.2 −6.2	^{194}Pt	1.1 −8.6
^{34}S	7.9 −2.6	^{64}Zn	7.3 −2.6	^{102}Ru	3.3 −5.9	^{200}Hg	0.9 −8.8
^{40}Ar	5.4 −4.1	^{66}Zn	5.7 −3.9	^{108}Pd	2.3 −6.5	^{208}Pb	0.7 −9.3
^{42}Ca	6.3 −1.6	^{68}Zn	4.4 −5.2	^{114}Cd	1.9 −6.8	^{226}Ra	2.2 −11.1
^{41}Ca	5.6 −3.2	^{72}Ge	5.7 −4.9	^{120}Sn	1.5 −7.2	^{232}Th	1.9 −11.2
^{46}Ca	5.1 −4.9	^{74}Ge	4.3 −6.2	^{130}Te	1.8 −8.9	^{238}U	1.7 −11.2
^{48}Ca	4.7 −6.5	^{78}Se	3.2 −6.2	^{132}Xe	1.8 −7.9	^{242}Pu	1.8 −10.7
^{48}Ti	6.7 −3.0	^{84}Kr	4.8 −6.4	^{138}Ba	1.8 −8.3	^{244}Cm	1.9 −10.8
^{52}Cr	7.4 −2.9	^{88}Sr	3.8 −6.0	^{140}Ce	1.7 −7.4		

Note. The energies are measured from the ground state of the target nucleus.

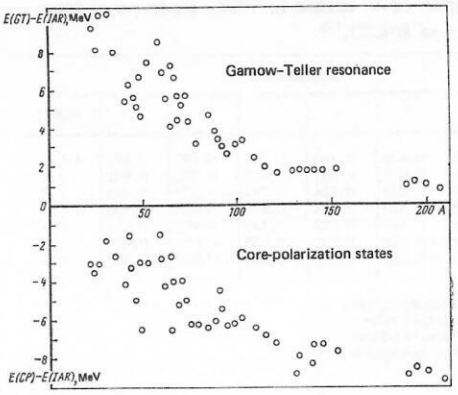

FIG. 28. Results of calculations of the positions of the Gamow–Teller resonance and core-polarization states.[103]

2. The value of B(GT) for the Gamow–Teller resonance increases smoothly with increasing A and is about $3(N-Z)$ in accordance with the sum rule.

3. The core-polarization state is situated about 4–9 MeV below the analog of the ground state. The intensity of its population in nuclei with $A = 100$–200 is B(GT) = 1.5.

4. The ratio of the reduced matrix elements of the Gamow–Teller transitions for population of the Gamow–Teller resonance and core-polarization states decreases with increasing A from 0.1 to about 0.01.

5. For a given element, the distance from the analog to the Gamow–Teller resonance decreases with increasing neutron deficit, while B(GT) increases.

As an example, we give the results of calculations for ^{94}Zr and ^{208}Pb. In Table XV, we give the energies of the 1^+ states in ^{94}Nb calculated from the analog of the ^{94}Zr ground state, the wave functions of these states, and B(GT). In Table XVI, the same data are given for ^{208}Bi.

The energy position of the Gamow–Teller resonance is well reproduced in this model. Experimental data are known[99] for ^{48}Ca. The Gamow–Teller resonance is situated at energy 11 MeV in ^{48}Se, or 4.4 MeV above the analog of the ^{48}Ca ground state. The calculation gives

TABLE XV. Energies of 1^+ states in ^{94}Nb, their wave functions, and the values of B(GT).[103]

E, MeV	Configuration			B (GT)
	1	2	3	
2.68	0.464	0.364	0.806	39.6
−4.52	0.246	0.822	−0.513	0.9
−6.34	0.850	−0.437	2.293	1.5

1 — $[g_{9/2}(p)\, g_{9/2}(n^{-1})]_{1^+}$;
$[d_{5/2}(p)\, d_{5/2}(n^{-1})]_{1^+}$;
2 — $[d_{3/2}(p)\, d_{5/2}(n^{-1})]_{1^+}$;
3 — $[g_{7/2}(p)\, g_{9/2}(n^{-1})]_{1^+}$.

TABLE XVI. Energies of 1^+ states in ^{208}Bi, their wave functions, and the values of $B(GT)$.[103]

E, MeV	Configuration							$B(GT)$
	1	2	3	4	5	6	7	
0.72	0.244	0.166	0.526	0.193	0.347	0.495	0.482	119.7
−7.16	0.029	0.024	0.084	0.037	0.107	0.579	−0.802	0.3
−8.18	0.072	0.060	0.238	0.124	0.711	−0.575	−0.286	1.2
−9.27	0.116	0.109	0.530	0.504	−0.577	−0.268	−0.185	1.5
−9.88	0.073	0.078	0.512	0.829	−0.153	−0.102	−0.075	0.4
−11.35	0.088	0.962	−0.248	−0.040	−0.038	−0.034	−0.027	0.1
−12.30	0.953	−0.156	−0.236	−0.054	−0.060	−0.058	−0.047	0.6

1 — $(f_{7/2}p^{-1}_{5/2}n)_{1^+}$;
2 — $(p_{3/2}p^{-1}_{1/2}n)_{1^+}$;
3 — $(f_{7/2}p^{-1}_{7/2}n)_{1^+}$; $(f_{5/2}p^{-1}_{5/2}n)_{1^+}$; $(h_{9/2}p^{-1}_{9/2}n)_{1^+}$; $(i_{13/2}p^{-1}_{13/2}n)_{1^+}$; $(p_{3/2}p^{-1}_{3/2}n)_{1^+}$; $(p_{1/2}p^{-1}_{1/2}n)_{1^+}$;
4 — $(p_{1/2}p^{-1}_{3/2}n)_{1^+}$;
5 — $(f_{5/2}p^{-1}_{7/2}n)_{1^+}$;
6 — $(h_{9/2}p^{-1}_{11/2}n)_{1^+}$;
7 — $(i_{11/2}p^{-1}_{13/2}n)_{1^+}$.

the value 4.72 MeV. For ^{90}Zr,[100] the Gamow–Teller resonance is situated in ^{90}Nb at excitation energy 3.6 MeV above the analog. The calculation gives the value 3.35 MeV. For ^{208}Pb in accordance with Ref. 24, the Gamow–Teller resonance is observed 0.4 MeV above the analog. The calculated value is 0.7 MeV. The calculated values of the energy difference $E(GT) - E(IAR)$ as a function of $(N-Z)/A$ are given in Fig. 29. The continuous straight line is drawn through all the points:

$$E(GT) - E(IAR) = \left[-\frac{50.2}{A}(N-Z) + 11.0 \right] \text{MeV}.$$

It can be seen that the position of the Gamow–Teller resonance depends strongly on the shell structure and is described by a straight line only on the average. The broken straight line is plotted in accordance with the experimental data of Ref. 102. It can be seen that the straight line gives a good description of the energies for the isotopes measured in Ref. 102. However, for a final decision with regard to the energy of the Gamow–Teller resonance measurements for a larger group of nuclei are needed.

The $B(GT)$ values for the Gamow–Teller resonance are known for ^{90}Zr (Ref. 100) and ^{208}Pb (Ref. 24) and are 8.3 and 48, respectively. The calculated values exceed the experimental values by about three times.

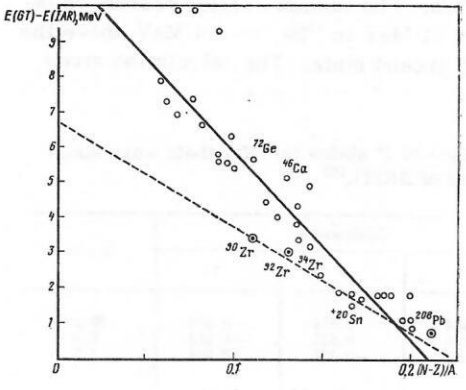

FIG. 29. Dependence of the position of the Gamow–Teller resonance on $(N-Z)/A$.[103]

Overall, the model correctly describes the experimental data on the (p,n) reaction. The interpretation of the peaks in the neutron spectra based on the microscopic approach to charge-exchange excitations appears more correct than the interpretation of Refs. 99–101, which take as their point of departure the existence of the $M1$ resonance in the target nucleus, its analog being interpreted as a $T_>$ state of the Gamow–Teller resonance. Strictly, the Gamow–Teller resonance is interpreted as the antianalog of the $M1$ resonance. This interpretation encounters serious difficulties in the analysis of the configurations that form the resonances. In addition, it is now clear that the $M1$ resonance is strongly suppressed in heavy nuclei, whereas the Gamow–Teller resonance exists.

In this section, we have discussed (p,n)-reaction experiments in which the Gamow–Teller resonance is excited in the final nucleus. It is natural to consider how the properties of the Gamow–Teller resonance are manifested in the compound nucleus. This question is considered in Ref. 19, in which it is shown that the Gamow–Teller resonance in the compound nucleus can be manifested as intermediate structure in proton resonances.

CONCLUSIONS

The experimental data and theoretical calculations considered in the present review lead to the unambiguous conclusion that a resonance energy structure exists in the β-decay strength functions. The main maximum in the strength functions (the Gamow–Teller resonance) is a special case of charge-exchange nuclear excitations. The accumulation of experimental data and the development of theoretical calculations on the properties of the Gamow–Teller resonance give information about the isovector parts of the effective nuclear interactions. It is of great interest to make experimental and theoretical investigations of charge-exchange excitations of other types (1^-, 2^+, etc.) and also to investigate the excitation of the Gamow–Teller resonance in heavy-ion reactions.

The energy structure of the β-decay strength functions may be extremely important in the analysis of various delayed processes, in calculations of astrophysical processes, and in various technological applications. It is therefore important to develop reliable methods for calculating the β-decay strength functions for different regions of nuclei and for calculating the half-lives of nuclei far from the stability band.

[1] P. G. Hansen, Adv. Nucl. Phys. **7**, 159 (1973).
[2] C. Gaarde *et al.*, Nucl. Phys. **A143**, 497 (1970).
[3] Yu. V. Naumov and O. E. Kraft, Fiz. Elem. Chastits At. Yadra **6**, 892 (1975) [Sov. J. Part. Nucl. **6**, 361 (1975)].
[4] Yu. V. Naumov *et al.*, Fiz. Elem. Chastits At. Yadra **9**, 1282 (1978) [Sov. J. Part. Nucl. **9**, 502 (1978)].
[5] V. A. Karnaukhov, Fiz. Elem. Chastits At. Yadra **4**, 1018 (1973) [Sov. J. Part. Nucl. **4**, 416 (1973)].
[6] R. R. Doering *et al.*, Phys. Rev. Lett. **35**, 1691 (1975).
[7] K.-L. Kratz *et al.*, Phys. Lett. **B65**, 231 (1976); Nucl. Phys. **A317**, 335 (1979).

[8]A. A. Bykov *et al.*, Preprint No. 628 [in Russian], Leningrad Institute of Nuclear Physics (1980).
[9]G. D. Alkhazov *et al.*, Pis'ma Zh. Eksp. Teor. Fiz. **32**, 68 (1980) [JETP Lett. **32**, 63 (1980)].
[10]A. A. Bykov *et al.*, Preprint No. 647 [in Russian], Leningrad Institute of Nuclear Physics (1981).
[11]A. Bohr and B. R. Mottelson, Nuclear Structure, Vol. 2, Benjamin, Reading, Mass. (1975) (Russian translation published by Mir, Moscow (1977)).
[12]Yu. V. Naumov and O. E. Kraft, Izospin v yadernoĭ fizike (Isospin in Nuclear Physics), Nauka, Leningrad (1972).
[13]V. P. Aleshin, Izv. Akad. Nauk SSSR, Ser. Fiz. **37**, 101 (1973).
[14]Yu. V. Naumov, Izv. Akad. Nauk SSSR, Ser. Fiz. **39**, 1646 (1975).
[15]O. Bohr and B. R. Mottelson, Nuclear Structure, Vol. 1, Benjamine, New York (1969) (Russian translation published by Mir, Moscow (1971)).
[16]J. Fujita, Y. Futami, and K. Ikeda, Prog. Theor. Phys. **38**, 107 (1967).
[17]Yu. V. Gaponov and Yu. S. Lyutostanskiĭ, Yad. Fiz. **19**, 62 (1974) [Sov. J. Nucl. Phys. **19**, 33 (1974)].
[18]H. V. Klapdor, Phys. Lett. **B65**, 35 (1976).
[19]A. A. Bykov *et al.*, Izv. Akad. Nauk SSSR, Ser. Fiz. **45**, 822 (1981); Preprint R15-80-786 [in Russian], JINR, Dubna (1980).
[20]K. Takahashi, M. Yamada, and T. Kondon, At. Data Nucl. Data Tables **12**, 101 (1973).
[21]A. A. Bykov and Yu. V. Naumov, Izv. Akad. Nauk SSSR, Ser. Fiz. **42**, 1911 (1978).
[22]B. F. Petrov and Yu. V. Naumov, Izv. Akad. Nauk SSSR, Ser. Fiz. **42**, 1918 (1978).
[23]C. D. Goodman *et al.*, Newsletter IUCF, No. 26 (1980).
[24]D. J. Horen *et al.*, Phys. Lett. **B95**, 27 (1980).
[25]E. Roeckl *et al.*, Z. Phys. **A294**, 221 (1980).
[26]V. G. Solov'ev, Teoriya slozhnykh yader, Nauka, Moscow (1971); English translation: Theory of Complex Nuclei, Pergamon Press, Oxford (1976).
[27]K. Ikeda, Prog. Theor. Phys. **31**, 434 (1964); J. Fujita and K. Ikeda, Nucl. Phys. **67**, 1451 (1965).
[28]R. A. Sorensen, Ark. Fys. **36**, 657 (1965); R. A. Sorenson, Nuclear Structure Dubna Symposium, Vol. 27, IAEA, Vienna (1968); J. Hablieb and R. A. Sorensen, Nucl. Phys. **A98**, 542 (1967).
[29]S. J. Gabrakov, A. A. Kuliev, and N. I. Piatov, Phys. Lett. **B36**, 275 (1971).
[30]Yu. V. Gaponov and Yu. S. Lyutostenskiĭ, Fiz. Elem. Chastits At. Yadra **12**, 1324 (1981) [Sov. J. Part. Nucl. **12**, 528 (1981)].
[31]S. Krewald *et al.*, Phys. Rev. Lett. **46**, 103 (1981).
[32]G. V. Klapdor *et al.*, Izv. Akad. Nauk SSSR, Ser. Fiz. **42**, 64 (1978).
[33]I. N. Izosimov and Yu. V. Naumov, Izv. Akad. Nauk SSSR, Ser. Fiz. **42**, 2248 (1978); H. V. Klapdor *et al.*, Phys. Lett. **B78**, 20 (1978).
[34]Yu. V. Naumov *et al.*, Preprint D7-80-556 [in Russian], JINR, Dubna (1980), p. 55.
[35]S. P. Ivanova, A. Kuliev, and D. I. Salamov, Yad. Fiz. **24**, 278 (1976) [Sov. J. Nucl. Phys. **24**, 145 (1976)]; S. P. Ivanova, A. Kuliev, and D. I. Salamov, Preprint R4-8972 [in Russian], JINR, Dubna (1975).
[36]D. R. Bes and Yi-Chung Cho, Nucl. Phys. **86**, 581 (1966).
[37]K. Aleklett, G. Nyman, and G. Rudstam, Nucl. Phys. **A246**, 425 (1975).
[38]P. Hornshoj *et al.*, Nucl. Phys. **A239**, 15 (1975).
[39]C. L. Duke *et al.*, Nucl. Phys. **A151**, 609 (1970).
[40]P. Hornshoj *et al.*, Nucl. Instrum. Methods **104**, 263 (1972).
[41]A. A. Bykov *et al.*, Izv. Akad. Nauk SSSR, Ser. Fiz. **44**, 918 (1980).
[42]V. A. Karnaukhov and L. A. Petrov, Yadra, udalennye ot polosy β-stabil'nosti (Nuclei Far from the β-Stability Band), Energoizdat, Moscow (1981).
[43]J. C. Hardy, CERN Report 76-13 (1976), p. 267.
[44]B. Jonson *et al.*, CERN Report 76-13 (1976), p. 277.
[45]P. Hornskoj *et al.*, Nucl. Phys. **A187**, 637 (1972).
[46]E. Nolte and H. Hick, Phys. Lett. **B97**, 55 (1980).
[47]D. D. Bogdanov, V. A. Karnaukhov, and L. A. Petrov, Yad. Fiz. **18**, 3 (1973) [Sov. J. Nucl. Phys. **18**, 1 (1973)]; Preprint R6-6861 [in Russian], JINR, Dubna (1973).
[48]V. A. Karnaukhov *et al.*, Nucl. Phys. **A90**, 23 (1967).
[49]E. Hagberg *et al.*, Nucl. Phys. **A208**, 309 (1973).
[50]P. Hoenshoj *et al.*, Nucl. Phys. **A187**, 539 (1972).
[51]D. D. Bogdanov *et al.*, Preprint R6-8962 [in Russian], JINR, Dubna (1975); Yad. Fiz. **24**, 9 (1976) [Sov. J. Nucl. Phys. **24**, 4 (1976)].
[52]D. D. Bogdanov *et al.*, Nucl. Phys. **A275**, 229 (1977); Preprint E6-9937 [in English], JINR, Dubna (1976).
[53]Y. Nir-El and S. Amiel, Report 76-13, CERN (1976), p. 322.
[54]K. L. Kratz *et al.*, Preprint D-6900, Max-Planck Institute für Kernphysik (1978).
[55]K. L. Kratz *et al.*, Phys. Lett. **B86**, 21 (1979).
[56]W. Knupfer, M. Dillig, and A. Richter, Phys. Lett. **B95**, 349 (1980).
[57]J. C. Hardy, B. Jonson, and P. G. Hansen, Nucl. Phys. **A305**, 15 (1978).
[58]J. C. Hardy *et al.*, Phys. Lett. **B71**, 307 (1977).
[59]V. I. Kuznetsov, N. K. Skobelev, and G. N. Flerov, Yad. Fiz. **4**, 279 (1966) [Sov. J. Nucl. Phys. **4**, 202 (1967)].
[60]L. G. Belov *et al.*, Preprint R15-9795 [in Russian], JINR, Dubna (1976).
[61]D. Habs *et al.*, Z. Phys. **A285**, 53 (1978).
[62]H. V. Klapdor *et al.*, Z. Phys. **A292**, 249 (1979).
[63]H. V. Kapdor *et al.*, in: Physics and Chemistry of Fission, Proc. of a Symposium, Vol. 1, July (1980), p. 175.
[64]S. P. Ivanova *et al.*, Fiz Elem. Chastits At. Yadra **7**, 450 (1976) [Sov. J. Part. Nucl. **7**, 175 (1976)].
[65]P. Möller and Y. R. Nix, in: Proc. of the Third IAEA Symposium on the Physics and Chemistry of Fission, Vol. 1, p. 103.
[66]P. Glassel, H. Rosler, and H. J. Specht, Nucl. Phys. **A256**, 220 (1976).
[67]I. N. Izosimov and Yu. V. Naumov, in: Tezisy XXXI Soveshchaniya po yadernoĭ spektroskopii i strukture atomnogo yadra, Samarkand (Abstracts of the 31st Symposium on Nuclear Spectroscopy and Nuclear Structure, Samarkand), Nauka, Leningrad (1981).
[68]B. B. Back *et al.*, Phys. Rev. C **9**, 1924 (1974).
[69]J. L. Lynn and B. B. Back, J. Phys. A **7**, 395 (1974).
[70]Yu. P. Gangrskiĭ *et al.*, Preprint R15-10613 [in Russian], JINR, Dubna (1977).
[71]L. Kh. Batist *et al.*, Preprint No. 363 [in Russian], Leningrad Institute of Nuclear Physics (1977)
[*Translation Editor's Note.* Reference 72 is missing in the Russian original.]
[73]M. Di Toro, Lett. Nuovo Cimento **22**, 608 (1978).
[74]A. V. Ignatyuk, N. S. Rabotnov, and G. Smirenkin, Phys. Lett. **B29**, 209 (1969).
[75]E. M. Burbidge *et al.*, Rev. Mod. Phys. **29**, 547 (1957).
[76]C. O. Wene, Astron. Astrophys. **44**, 233 (1975).
[77]D. N. Schramm and W. A. Fowler, Nature **231**, 103 (1971).
[78]C. O. Wene and S. A. E. Johansson, Phys. Scr. **A10**, 156 (1974).
[79]T. Ohnishi, Astrophys. Space Sci. **58**, 149 (1978).
[80]D. N. Schramm and G. S. Wasserbyrg, Astrophys. J. **162**, 57 (1970).
[81]H. V. Klapdor and C. O. Wene, Astrophys. J. Lett. **230**, L113 (1979).
[82]P. A. Seeger *et al.*, Astrophys. J. Suppl. **11**, 121 (1965).
[83]D. N. Schramm, Astrophys. J. **185**, 293 (1973).
[84]J. B. Black and D. N. Schramm, Astrophys. J. **209**, 846 (1976).

[85]T. Kodama and K. Takahashi, Nucl. Phys. **A239**, 489 (1975).
[86]I. N. Izosimov and Yu. V. Naumov, in: Tezisy XXX Sove Soveshchaniya po yadernoĭ spektroskopii i strukture atomnogo yadra, Leningrad (Abstracts of the 30th Symposium on Nuclear Spectroscopy and Nuclear Structure, Leningrad), Nauka, Leningrad (1980).
[87]D. N. Schramm, Ann. Rev. Astron. Astrophys. **12**, 383 (1975).
[88]C. D. Goodman *et al.*, IEEE Trans. Nucl. Sci. **26**, 2248 (1979).
[89]C. D. Goodman *et al.*, Nucl. Instrum. Methods **151**, 125 (1978).
[90]C. D. Goodman *et al.*, IEEE Trans. Nucl. Sci. **25**, 577 (1978).
[91]C. A. Goulding *et al.*, Nucl. Phys. **A331**, 29 (1979).
[92]J. D. Anderson, C. Wong, and V. A. Madsen, Phys. Rev. Lett. **24**, 1074 (1970).
[93]W. A. Sterrenburg *et al.*, Phys. Lett. **B91**, 337 (1980).
[94]C. D. Goodman *et al.*, Phys. Rev. Lett. **44**, 1755 (1980).
[95]G. R. Satchler, Nucl. Phys. **55**, 1 (1964).
[96]A. K. Kerman *et al.*, Ann. Phys. (N.Y.) **8**, 551 (1959).
[97]F. Petrovich *et al.*, Phys. Rev. C **21**, 1718 (1980).
[98]G. E. Brown, J. Specht, and J. Wambach, Phys. Rev. Lett. **46**, 1057 (1981).
[99]B. D. Anderson *et al.*, Phys. Rev. Lett. **45**, 699 (1980).
[100]D. E. Bainum *et al.*, Phys. Rev. Lett. **44**, 1751 (1980).
[101]W. A. Sterrenburg *et al.*, Phys. Rev. Lett. **45**, 1839 (1980).
[102]D. J. Horen *et al.*, Phys. Lett. **B99**, 383 (1981).
[103]A. A. Bykov *et al.*, in: Tezisy XXXI Soveshchaniya po yadernoĭ spektroskopii i strukture atomnogo yadra, Samarkand (Abstracts of the 31st Symposium on Nuclear Spectroscopy and Nuclear Structure, Samarkand), Nauka, Leningrad (1981).
[104]E. G. Bilpuch *et al.*, Phys. Rep. **28**, 145 (1976).
[105]A. Lane, Ann. Phys. (N.Y.) **63**, 173 (1971).
[106]C. Mahoux and H. Weidenmüller, Nucl. Phys. **A130**. 481 (1969).
[107]W. Wells, E. Bilpuch, and G. Mitchell, Phys. Lett. **B86**, 18 (1979).

Translated by Julian B. Barbour